



UNIVERZITET U BEOGRADU
FIZIČKI FAKULTET

MASTER RAD

Fundamentalne strune, termalni horizonti i maksimalni haos

Autor:
Vladan Đukić

Mentori:
Dr Mihailo Čubrović
Prof Dr Voja
Radovanović

Septembar, 2023.
Beograd



UNIVERSITY OF BELGRADE
FACULTY OF PHYSICS

MASTER THESIS

Fundamental strings, thermal horizons and the chaos bound

Author:
Vladan Đukić

Supervisors:
Dr. Mihailo Čubrović
Prof. Dr. Voja
Radovanović

September, 2023
Belgrade

Sažetak

Proučena je dinamika probnih fundamentalnih struna u nekoliko pozadinskih geometrija: Anti de-Sitter-Švarcšildova, crna D3 brana i D1-D5-p crna struna. Iako je dinamika otvorenih struna u ovim geometrijama integrabilna, klasične jednačine kretanja imaju pozitivne Ljapunovljeve eksponente u blizini termalnog horizonta, zbog postojanja nestabilne sedlaste tačke. Ljapunovljev eksponent nerotirajućih struna dostiže Maldasena-Šenker-Stanfordovu (MSS) granicu ("maksimalni kaos"). Pokazano je da je to posledica delovanja generatora Lijeve algebre $\mathfrak{sl}(2)$ u okolini horizonta. Kod otvorene probne strune u pozadini D1-D5-p crne strune on odgovara vremenskoj skali termalizacije teškog kvarka u jako kuplovanoj kvark-gluonskoj plazmi, pošto se može povezati sa spektrom kvazi-normalnih moda, koje odgovaraju vremenskoj skali disipacije fluktuacija na fundamentalnoj struni. Dinamika rotirajućih zatvorenih struna je neintegrabilna, ali njihov Ljapunovljev eksponent nije povezan sa MSS granicom: one opisuju raspad vakuuma u dualnoj super-Jang-Milsovoj gejdž teoriji. Zaključak je da holografška interpretacija Ljapunovljevog eksponenta u asimptotski Anti de-Siterovim prostorima nije povezana sa kaosom, već sa neravnotežnim fluktuacijama u dualnoj teoriji polja.

Abstract

We study the dynamics of fundamental strings in Anti de-Sitter Schwarzschild, black D3 brane and D1-D5-p black string backgrounds in the probe limit. Despite the fact that the dynamics of open strings in these backgrounds is integrable, the classical equations of motion exhibit positive Lyapunov exponents near thermal horizons, due to an unstable saddle point. For non-spinning strings the Lyapunov exponents saturate the Maldacena-Shenker-Stanford (MSS) bound on chaos. We suggest that this is a consequence of the action of $\mathfrak{sl}(2)$ Lie algebra generators in the near-horizon region. For a straight open string in the D1-D5-p black string background it corresponds to the thermalization timescale of a heavy quark in strongly coupled quark-gluon plasma, since it can be related to the spectrum of quasi-normal modes, i.e. the decay rates of the fundamental string fluctuations. For spinning closed strings the dynamics is nonintegrable but the Lyapunov exponents are unrelated to the MSS bound: they describe the decay of an unstable vacuum in the super-Yang-Mills dual gauge theory. In conclusion, the holographic interpretation of the bulk Lyapunov exponent is not related to chaos but to off-equilibrium fluctuations of the dual field theory.

Acknowledgements

I would like to express my sincere gratitude to my supervisor, Dr. Mihailo Čubrović, for his invaluable guidance, unwavering support, and insightful discussions throughout the course of this research. His expertise and dedication have been instrumental in shaping the direction and quality of this thesis. I am truly fortunate to have had the opportunity to learn from his wisdom and experience.

I extend my heartfelt appreciation to my family for their support and encouragement during this challenging yet fulfilling journey.

Contents

1	Introduction	2
2	Overture: particles and shock waves in AdS	6
2.1	A particle in AdS and its holographic dual	6
2.1.1	Kink from a bulk particle in AdS and BTZ background	6
2.1.2	Shock waves from OTOC calculation	8
3	Static open string in black hole background	12
3.1	AdS Schwarzschild back hole: setup	12
3.1.1	Nambu-Goto action	12
3.1.2	Polyakov action	13
3.2	Integrability in AdS-Schwarzschild	15
3.3	Lyapunov exponent near the AdS-Schwarzschild horizon	17
3.4	Lyapunov exponent near a general hyperscaling-violating horizon	18
4	Intermezzo: Static open string in black brane backgrounds	19
4.1	Extremal black D3 brane	19
4.2	Non-extremal black D3 brane	21
4.3	Numerical solutions	22
5	Open string in D1-D5-p black string background	23
5.1	Introduction	23
5.2	Setup	24
5.3	Analytic estimate of the Lyapunov exponent	26
5.3.1	Near-horizon limit	26
5.3.2	Far from horizon	28
5.4	Retarded Green's function in the static limit	28
5.5	Dynamics of transverse fluctuations	31
5.5.1	Near region: extremal case	32
5.5.2	Near region: near-extremal case	33
5.5.3	Signals of instability	36
5.5.4	Far region solution	37
6	Spectrum of rotating strings and energy-angular momentum relations	39
6.1	Introduction	39
6.2	Setup	40
6.2.1	Closed spinning string	40
6.2.2	Closed winding spinning string	42

6.3	Lyapunov exponents and the deformations of the gauge theory	43
6.3.1	Variational equations and their solutions	43
6.3.2	Deformations of the spectrum of the gauge operators	44
6.4	Discussion and conclusions	45
7	Discussion and conclusions	46
A	Trivial dynamics of time-dependent fluctuations	48
B	Symmetries of AdS₃ and BTZ spaces	49
C	Conserved charges in AdS₃ gravity	51

Chapter 1

Introduction

Chaos in string theory has traversed the way from an arcane and little-noticed topic to a mainstream field, thanks to the ideas of fast scrambling and black holes as the fastest scramblers in nature [1], the Maldacena-Shenker-Stanford (MSS) maximum chaos bound for strongly coupled field theories with black hole duals [2] and the notion of out-of-time ordered correlators (OTOC) [3, 4, 5] and their applications in the physics of chaotic strongly coupled systems [6, 7, 8]. An important motor of the field is also the connection to recent progress on the black hole information problem [9, 10, 11, 12] and the related puzzle of factorization [13, 14, 15, 16, 17, 18, 19, 20]. The guiding idea through all these topics is of course the AdS/CFT duality, the unifying principle of many topics in string theory and gravity. Our primary interest thus lies in the dynamics in asymptotically AdS backgrounds.

The current paradigm of holographic chaos starts by noticing that a perturbation of the black hole horizon has universal dynamics determined solely by the temperature of the horizon: thanks to the infinite redshift, all details of the perturbation become macroscopically invisible within a time of order $\sim 1/T$ where T is the Hawking temperature. This is called scrambling: the information is there but it takes very long time (or many qubits of Hawking radiation) to reconstruct it. The holographic consequence of the fast scrambling idea is the universal timescale of quantum chaos. Quantizing the classical notion of exponential sensitivity to initial conditions, we can look at the operator $\epsilon [X(t), P(0)]$ where X and P can be understood as some conjugate pair of a generalized coordinate and momentum operator. Since P generates translations, the meaning of this object is that at time zero we shift X by ϵ and then let it evolve for time t . The commutator itself is in general complex, but the square of its module $|[X(t), P(0)]|^2$ (dropping the irrelevant constant ϵ) is a real quantity that should show exponential growth. This is indeed what happens for AdS black holes and their strongly coupled, large- N CFT duals: the square of the commutator (usually called OTOC) shows universal growth $\sim \exp(2\lambda_L t)$ where the quantum Lyapunov exponent $\lambda_L = 2\pi T$ is known as the MSS bound or the chaos bound: it is the maximum possible value according to the fast scrambling result [1, 2].

We shall not discuss in any detail those aspects of the fast scrambling which do not directly concern this thesis. What we aim for is a better understanding of the connection between the bulk dynamics in black hole backgrounds and dual field theory: the shock wave perturbations which determine the OTOC are but one of many probes whose orbits we can study in the bulk. How is all this bulk information encoded in field theory? This is the main motivation of this work.

Among the many questions which have opened up, there is one seemingly technical but

in fact physically important subtlety. Several papers have reported the saturation of the MSS bound for *bulk* orbits of particles [21, 22], or its slight modification/generalization for fields [21] and strings [23, 24, 25]; the systematic answer to the question of the bulk Lyapunov exponent is given in [26]. However, a very simple question arises: *why should there ever be an MSS bound for bulk Lyapunov exponents?* The OTOC exponent and its MSS bound $\lambda = 2\pi T$ in principle have no simple relation to the classical bulk motion and its Lyapunov exponent: the former is a property of a time-dependent correlation function in dual CFT, determined by a 4-wave scattering amplitude in the bulk, and the latter is the solution of a bulk equation of motion, for a single orbit, with no scattering and thus no OTOC-like interpretation in the bulk. This relates to a more general question: what is the CFT dual of a bulk orbit (and its Lyapunov instability exponent)? Some important work was done on this issue [27, 28, 29, 30, 31, 32], and the outcome is that a bulk particle is dual to a shock wave perturbation of the dual CFT. But many details are still missing; in particular, the answer cited above holds for a geodesic with both endpoints on the AdS boundary; it is less clear what the CFT dual is for an orbit not reaching the boundary.

Paradoxically, a string in the bulk, specifically an open string, is perhaps an easier case for study. It is long known that a static or dragging string, with one endpoint in the interior and the other on the boundary, is dual to a heavy quark in the quark-gluon plasma of the supersymmetric Yang-Mills gauge theory [33, 34]. Likewise, an open string with both endpoints on the boundary represents a quark-antiquark pair [35, 36, 37, 38, 39], and encodes information on the confinement mechanism. It is thus a convenient framework to pose our main question: *what is the meaning of the bulk Lyapunov exponent and what does it have to do with the MSS bound?*

In this work we give a partial answer to the question and demonstrate it by a number of case studies involving bosonic open strings in various backgrounds.¹ There is, in fact, no unique answer to the question of the CFT dual to a Lyapunov exponent: just as various string configurations have various field theory duals (a quark, a bound pair of quarks, an EPR pair, an accelerating quark...), likewise the Lyapunov stability of these different solutions will have different meanings. Furthermore, on the string worldsheet there are two coordinates thus we have two Lyapunov exponents, with different CFT meanings.

Our leading idea is that the variational equation that determines the Lyapunov exponent is really the second variation of the classical action (the first variation yields the equations of motion for the string itself, the second variation for its Lyapunov exponent). The second variation can then be added to the on-shell action, allowing us to identify the variation of the classical solution with a two-point correlation function (similar to how the solution itself determines a two-point function through the usual dictionary of the gauge/string duality [40, 41]). If the variation is over the worldsheet time, it typically corresponds to time-dependent response function in field theory, describing the behavior of the quark under an external (momentary) kick. If the variation is over the compact (spacelike) worldsheet coordinate (along the string), the Lyapunov exponent rather has the meaning of the energy/renormalization group (RG) scale on which the flows toward different infrared (IR) fixed points start to diverge, and describes the scale of off-equilibrium fluctuations.

We also find that the MSS form of the exponent is really a red herring: in the strict

¹While the dynamics of a superstring would be an interesting problem to study, in this work we stick solely to the bosonic sector. This is enough to understand the principles, and also to model holographically the dynamics of a heavy quark in Yang-Mills plasma.

infinite-coupling, infinite- N limit, $2\pi T$ becomes a natural scale which has to appear in all fluctuation equations. As soon as we decrease symmetry (e.g. by considering a D1-D5-p bound state in the bulk that breaks rotational invariance) or include stringy effects, the bulk exponent (as well as OTOC [5] and other CFT correlation functions) undergo corrections, and do not coincide anymore (neither among themselves nor with the MSS bound). Recent work on universal near-horizon symmetries [42, 43] has shone additional light on the issue, allowing us to view the MSS scale as the fundamental property of black hole horizons, so it can appear in any CFT correlator which is sensitive to temperature T , i.e. which probes the energy scales smaller than T . The puzzle of "why $2\pi T$ pops out everywhere" is thus a fake issue: it disappears as soon as leading corrections are taken into account.

Our results so far have a quality of a collection of solid examples and calculations unified by a somewhat handwaving general idea. Nevertheless, we feel that we now understand much better the origin of the MSS expression $2\pi T$ in bulk dynamics, and also the reason why its connection to chaos is fake.² We want to argue that the study of chaotic dynamics of geodesics and strings in holographic backgrounds is a fruitful field which can still show surprises, but one has to be careful about the field theory interpretation, which is not as simple as previously thought.

The plan of the thesis is the following.

- In Chapter 2 we motivate our research and some of the conclusions by considering point particles and their orbits (geodesics) and their holographic meaning: these are for the most part known results but we show them in a novel light, demonstrating that the chaos bound appears generically when considering orbits and their instabilities, without actual connection to chaos.
- In Chapter 3 we introduce the static open string in AdS-Schwarzschild (AdSS) spacetime and describe the fluctuations along the string. We discuss the integrability of this system and also introduce the analytic method by which we estimate the Lyapunov exponent from the near-horizon variational equation of the string. We find that the MSS bound is saturated by the bulk Lyapunov exponent both in AdSS and in a general hyperscaling-violating extension of black holes in AdS.
- In Chapter 4, as a warm-up exercise for the Chapter 5, we extend our study of static open string to the black D3 brane background and find that the universal MSS bound is still saturated. This gives a hint as to its meaning.
- In Chapter 5 we discuss some of the most important results of our work. We begin with a brief review of some nice features of D1-D5-p black string geometry and apply our near-horizon analytic method to estimate the Lyapunov exponent in this background. We find that the Lyapunov exponent is modified in rotating backgrounds. In the non-rotating limit we recover the universal MSS bound value. We continue our discussion in the spirit of Chapter 2, studying the time-dependent dynamics of transverse fluctuations along the string and calculating the retarded Green's function in the IR region in absence of rotation, where we find how the MSS scale emerges naturally in the resulting propagator. We study the poles of

²It is fake in our context, where it appears as a bulk Lyapunov exponent. In the OTOC calculation, its relation to chaos is undisputable.

the retarded Green's function, find how the Lyapunov exponent is related to the spectrum of quasi-normal modes and discuss its implications for the interpretation of the bulk Lyapunov exponent in situations where bulk chaos is not present, but the MSS bound is saturated.

- In Chapter 6 we consider a very different system – closed spinning strings in $\text{AdS}_5 \times \mathbb{S}^5$ spacetime, the celebrated testing ground for holography where holographically computed dispersion relations for heavy operators can be compared to gauge theory results at strong coupling. This is a time-dependent and horizon-less setup which shows the meaning of bulk Lyapunov exponents as tracing the RG flow in field theory from an unstable to a stable fixed point.
- In Appendix A we briefly consider time-dependent configurations of open strings instead of spatial fluctuations that we focus on in most of the thesis and show that time-dependent dynamics is trivial; the sole interesting aspect is the spatial configuration.
- In Appendix B we review the algebra of Killing vectors in AdS_3 and non-rotating BTZ spacetimes. We show how they are related to the $\mathfrak{sl}(2)$ Lie algebra that is essential for understanding the universality of the MSS bound $2\pi T$ even in integrable systems.
- In Appendix C we use the Brown-York tensor to derive total energy and angular momentum of the rotating BTZ black hole that we encounter in the near-horizon limit of near-extremal D1-D5p black string.

Chapter 2

Overture: particles and shock waves in AdS

2.1 A particle in AdS and its holographic dual

As we have argued in the Introduction, the open string with one end at the boundary (i.e., a heavy quark in thermal plasma) is the simplest setup for exploring the meaning of the bulk Lyapunov exponent. However, it is instructive to briefly sketch the case of geodesics, i.e. point particle orbits in the bulk. Several works have explored specifically the Lyapunov exponent of particle orbits, mainly at the black hole horizon, obtaining the MSS value $\lambda = 2\pi T$ in most cases [22, 44] but there are exceptions [21, 25]. Crucially, the analysis in [26] has shown that the variational equation of an orbit circumventing the horizon of a fairly generic black hole indeed predicts the MSS value for the exponent, however that need not be the maximum value (i.e., away from the horizon one might obtain a larger value). Therefore, this bulk geodesic chaos is neither necessarily maximal, nor obviously connected to quantum chaos in the dual CFT. So what is its meaning? A full answer is beyond the scope of this paper – bulk geodesics correspond to insertions of heavy operators in CFT, and it is not clear how to interpret the variational equations in the bulk, i.e. the divergence rate of orbits.

On a qualitative level however we can argue that the variation of a bulk geodesic represents simply a non-equilibrium correlator in dual CFT, in a state corresponding to a point particle in the bulk. The bulk response to such a source is a non-analyticity (a wedge) in the geometry. A similar thing appears (with very different boundary conditions) in the calculation of OTOC in dual CFT [5], where the bulk metric develops a shock wave, i.e. again a discontinuity, as backreaction from pointlike particles (waves in eikonal approximation) at the horizon. Roughly for this reason the variation of the bulk equation of motion in black hole backgrounds exhibits the same exponential growth (with the MSS rate) as the four-wave eikonal scattering, even though the physics differs. In order to show this, we first review the known results on the dual meaning of a bulk particle.

2.1.1 Kink from a bulk particle in AdS and BTZ background

The holographic meaning of a (massive) particle in the bulk is known [30, 31, 45, 46, 47]: it is a kink excitation of the dual field theory, localized in spacetime and highly delocalized in energy-momentum. Let us remind the reader how this works. Consider a heavy scalar

field of conformal dimension Δ in global AdS₃ spacetime with the metric:

$$ds^2 = (r^2 + 1) (-dt^2 + d\phi^2) + \frac{dr^2}{r^2 + 1}, \quad (2.1)$$

where t , ϕ and r correspond to time, angle on the boundary circle and the radial direction ($0 < r < \infty$). According to [30], the bulk-to-bulk propagator for a heavy scalar field between two points $x_1 = (t, r_1, \phi_1)$ and $x_2 = (t, r_2, \phi_2)$ is well-described in the eikonal approximation as a sum over the classical geodesic solutions g (there may be more than one) connecting the points:

$$\mathcal{G}(x_1; x_2) = \sum_g e^{-\Delta L_g(x_1, x_2)}, \quad (2.2)$$

where $L_g(x_1, x_2)$ is the length of the geodesic. Taking the points $x_{1,2}$ to the boundary, [30] obtain the CFT propagator $G(t, \phi_1; t, \phi_2)$ simply as the limit of Eq. (2.2) when $r_{1,2} \rightarrow \infty$.¹ In pure global AdS₃, the geodesic is unique and its length is

$$L = 2 \log \left(\frac{2 \sin(\phi_1 - \phi_2)}{\epsilon} \right), \quad (2.3)$$

where ϵ is the ultraviolet (UV) cutoff, i.e. we take $r_{1,2} = 1/\epsilon$ instead of infinity. Plugging this into Eq. (2.2) yields the expected two-point CFT correlator $G(t, \phi_1; t, \phi_2) = 1/(2 \sin(\phi_1 - \phi_2))^{2\Delta}$.

Consider now a point particle of mass m in AdS₃. Such a particle introduces a wedge in spacetime by its backreaction (its stress-energy tensor is proportional to a Dirac delta as shown in [28]). Therefore, the leading $1/N$ effect from the massive particle will modify the result (2.3) as we now have to look at the global AdS₃ with an excised wedge of defect angle $2\pi - 2\gamma$, where γ is related to the particle mass m as $\gamma = \pi - m$. Now there are two geodesics between x_1 and x_2 , the first one outside the wedge and the second one passing through the tear in spacetime; which one is dominant (shorter) is determined by the relative magnitude of $\phi_1 - \phi_2$ and γ :

$$L^{(i)} = 2 \log \left(\frac{2 \sin(\phi_1 - \phi_2)}{\epsilon} \right), \quad 0 \leq \phi_1 - \phi_2 \leq \frac{\pi - \gamma}{2} \quad (2.4)$$

$$L^{(ii)} = 2 \log \left(\frac{2 \sin(\phi_1 - \phi_2 + \gamma)}{\epsilon} \right), \quad \frac{\pi - \gamma}{2} < \phi_1 - \phi_2 < \pi - \gamma. \quad (2.5)$$

Therefore, right at $\phi_1 - \phi_2 = \pi - \gamma$ there is a kink where the solutions meet. Parametrizing the geodesic by some proper time s as $\phi(s=0) = \phi_1$, $\phi(s=\pi) = \phi_2$ and inserting into (2.4-2.5), the kink can be expressed as

$$\frac{\partial \log G}{\partial s} \Big|_{\phi(s)=\pi-\gamma+} - \frac{\partial \log G}{\partial s} \Big|_{\phi(s)=\pi-\gamma-} = 2\Delta \tan \frac{\gamma}{2} \frac{\partial \phi(s)}{\partial s} \Big|_{\phi(s)=\pi-\gamma}. \quad (2.6)$$

The above can be generalized for non-equal-time geodesics (with $t_1 \neq t_2$) and for the BTZ black hole [31] by boosting the point x_2 and employing the method of images, respectively.

¹This is of course not obvious and does not in general work like this in AdS/CFT; detailed justification is found in [30].

The detailed account of how this works can be found in [31]. The outcome is that the bulk-to-bulk propagator in a BTZ background with the metric

$$ds^2 = -r^2 f(r) dt^2 + \frac{1}{r^2 f(r)} dr^2 + r^2 d\phi^2, \quad f(r) = 1 - \left(\frac{r_h}{r}\right)^2 \quad (2.7)$$

becomes a sum over images enumerated by n :

$$G(t_1, \phi_1; t_2, \phi_2) = \left(\frac{r_h}{2r}\right)^{2\Delta} \sum_{n=-\infty}^{\infty} \frac{1}{[\cosh(r_h(\phi_1 - \phi_2 + 2\pi n)) - \cosh(r_h(t_2 - t_1))]^\Delta}, \quad (2.8)$$

where r_h is the horizon radius. Here we already see the MSS scale, as $r_h = 2\pi T$ in the BTZ geometry. We have obtained it without any connection to chaos or OTOC – merely as the energy scale of a thermal, non-stationary correlation function.

2.1.2 Shock waves from OTOC calculation

The basic recipe for the calculation of OTOC in the large- N limit [1, 3, 4, 5] reduces to the calculation of backreaction from an infalling wave at late times. At late times, the wave is practically at the horizon and thus receives a huge redshift; evolving the wave back to the UV makes its energy very high, so that it can be considered as effectively classical, justifying the eikonal approximation. The latter is precisely equivalent to the backreaction from a particle (for localized shocks), or from a spherical shell (for spherical shocks) [27, 28]. We now work in Rindler-AdS₃ spacetime as it is the only exactly solvable case. However, we keep the factors $2\pi T$ even though $2\pi T = 1$ in Rindler-AdS, in order to see the MSS scale explicitly and bearing in mind that the scaling will remain valid also in more complicated geometries with a thermal horizon.

The wavefunction of an outgoing scalar field ψ of conformal dimension Δ with momentum p^V , propagating from the point at x in the bulk to the point (t_1, x_1) at the boundary, reads:

$$\psi(p^V, x; t, x_1) = \int dU e^{i\frac{p^V U}{2}} K_\Delta(U, V = 0, x; t_1, x_1) O(t_1, x_1), \quad (2.9)$$

where $O(t_1, x_1)$ is the value of ψ at the boundary, $K(U, V, x; t_1, x_1)$ is the bulk-to-boundary propagator from (U, V, x) to $(t_1, r = \infty, x_1)$, and p^V is the V -component of the momentum (conjugate to U). We use the standard Kruskal-Szekeres coordinates in the bulk (hence U, V appear instead of t, r). In the Rindler-AdS background, one can find the momentum-space propagator in analytic form as in [5]:

$$K_\Delta(p^V, x; t_1, x_1) = \frac{1}{(Ue^{2\pi T t_1} - Ve^{-2\pi T t_1} + \cosh(x - x_1))^\Delta} \quad (2.10)$$

which, upon plugging in into Eq. (2.9) and integrating over U (i.e., Fourier-transforming) yields the expression for the wavefunction:

$$\psi(p^V, x; t_1, x_1) = \Theta(p^V) \frac{2i\pi e^{-2\pi T t_1}}{\Gamma(\Delta)} (2ip^V e^{-2\pi T t_1})^{\Delta-1} e^{-2ip^V e^{-2\pi T t_1} \cosh(x-x_1)} \quad (2.11)$$

This is all familiar and can be found in [5] and earlier works; computing the wavefunctions for all four waves (two infalling and two outgoing) and computing their scattering amplitude yields the OTOC. But it has remained largely unnoticed that a single-wave

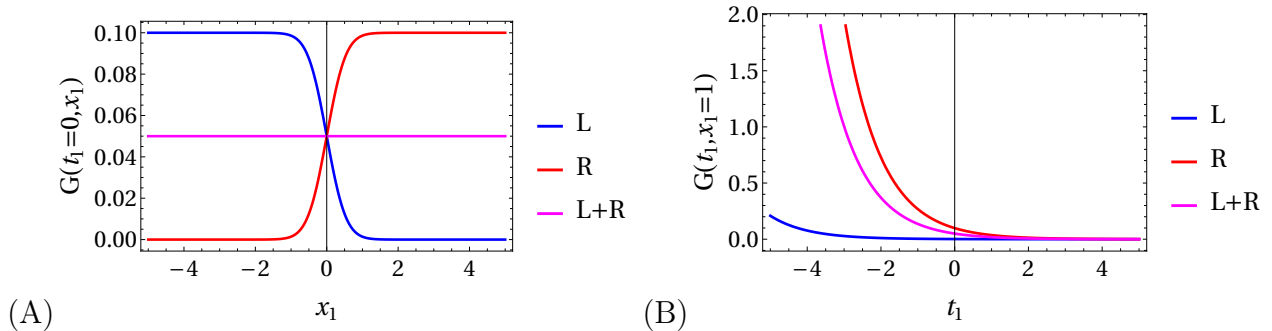


Figure 2.1: The single-operator amplitude $\langle O_1(t_1, x_1) \rangle$ in a black hole background (corresponding to a shock-wave fluctuation from a classical particle moving in the bulk) describes a one-point CFT correlation function $G(t_1, x_1)$, which consists from a kink (blue) and an antikink (red) located at $t = x = 0$; the amplitude decays exponentially with time $t > 0$ and the distance from zero $|x|$. The sum of the kink and antikink is a constant, as the expectation value of an operator in static and homogeneous background does not depend on time or location. We show the correlator at constant-time slice as a function of x (A) and at constant- x slice as a function of t (B). The temperature is $T = 1/2\pi$ and the conformal dimension is $\Delta = 5$.

amplitude, when there is no scattering (the outgoing wave is then just the continuation of the infalling wave), describes a kink excitation in dual CFT.

Let us start from a single insertion $\langle O_1(t_1, x_1) \rangle$, considering only the outgoing wave (2.11). This case is not very interesting physically, but it will serve to make a formal connection with the kink found for a massive particle in pure AdS. By definition, the bulk amplitude that determines the one-point function $\langle O_1(t_1, x_1) \rangle$ is given by

$$\langle O(t_1, x_1) \rangle = \int dx \int dp^V \psi(p^V, x; t_1, x_1) e^{-S_1}, \quad S_1 = \frac{1}{2} \int dx \sqrt{-g} h_{VV} T^{VV} = 0. \quad (2.12)$$

The on-shell action equals zero because there is no scattering – we only have a single wave which comes out from the horizon. We are left with the integral of the wavefunction in (2.12), yielding:

$$\begin{aligned} \langle O(t_1, x_1) \rangle &= 2i\pi e^{-2\pi T t_1} \frac{\Delta}{\Delta + 1} \left[\mathcal{A} e^{-(\Delta+1)x_1} {}_2F_1 \left(\frac{\Delta + 1}{2}, 1 + \Delta, \frac{3 + \Delta}{2}; -e^{-2x_1} \right) + \right. \\ &\quad \left. + \mathcal{B} e^{(\Delta+1)x_1} {}_2F_1 \left(\frac{\Delta + 1}{2}, 1 + \Delta, \frac{3 + \Delta}{2}; -e^{2x_1} \right) \right]. \end{aligned} \quad (2.13)$$

The two branches have coefficients $\mathcal{A} = \mathcal{B} = 1/2$ and correspond to the left- and right-moving kink, as shown in Fig. 2.1. Their sum is just a constant, i.e. the norm of the wave. Analyzing the hypergeometric functions in (2.13), one finds that the kink magnitude is exactly Δ – different from (2.6) but still a kink, now corresponding to an infalling particle instead of a static particle at $r = 0$. The time dependence already has the $2\pi T$ factor, but for the single-point function it is not very interesting, as we just have an exponential decay.

What happens if we consider a perturbation which falls from one boundary at (t_1, x_1) and arrives to the other boundary at (t_2, x_2) ?² Now we have two waves in the bulk, the

²Of course, physically all quantities are computed on the right boundary but we can represent each wave on any bulk slice for computational convenience.

outgoing wave (2.11) and the infalling wave

$$\psi(q^U, x'; t_2, x_2) = \Theta(q^U) \frac{-2i\pi e^{2\pi T t_2}}{\Gamma(\Delta)} (-2iq^U e^{2\pi T t_2})^{\Delta-1} e^{2iq^U e^{2\pi T t_2} \cosh(x'-x_2)}. \quad (2.14)$$

The resulting amplitude describes the propagation from the point (t_1, x_1) to the point (t_2, x_2) :

$$\langle O(t_1, x_1) O(t_2, x_2) \rangle = \int dx \int dx' \int dp^V \int dq^U \psi(p^V, x; t_1, x_1) \psi^*(q^U, x'; t_2, x_2). \quad (2.15)$$

The action S_1 is now nonzero as the two waves scatter off each other. In the eikonal approximation, one easily finds the result from the shock-wave solutions given in [28, 5]:

$$T^{VV} = g^{UV} g^{UV} T_{UU} = \frac{2}{r_h} p^V \delta(U) \delta(x - x_1), \quad h_{VV} = \frac{1}{2} p^U \delta(V) e^{-\sqrt{2\pi T r_h} |x|} \quad (2.16)$$

$$S_1 = \frac{1}{2} \int dx \sqrt{-g} h_{VV} T^{VV} = \frac{1}{r_h} p^U p^V. \quad (2.17)$$

We were unable to solve exactly the integral (2.15) with the above phase shift, but for long times $t_2 \gg t_1$ we can expand in $\exp(-2\pi T(t_2 - t_1))$ and obtain

$$\langle O(t_1, x_1) O(t_2, x_2) \rangle \sim 2\pi (1 + e^{2\pi T(t_2 - t_1)})^{-\Delta} {}_2F_1 \left(\frac{\Delta + 1}{2}, 1 + \Delta, \frac{3 + \Delta}{2}; -e^{-2|x_2 - x_1|} \right). \quad (2.18)$$

There is a kink solution in both time and space, with the time kink amplitude $r_h = 2\pi T$, the universal MSS scale (Fig. 2.2). This object – a single orbit in the bulk between the points (t_1, x_1) and (t_2, x_2) , which determines some two-point function $\langle O(t_1, x_1) O(t_2, x_2) \rangle$ – is found also in the calculation of the Lyapunov exponent. It shows the same universal scale, which in this context has little to do with chaos. At a purely formal level, it is guaranteed to appear in any particle/eikonal amplitude in the presence of thermal horizons.

In the next chapter we will introduce open strings and study their Lyapunov stability. Open strings are not pointlike objects hence they will not give rise to shock waves. Their correlation functions (in the bosonic sector) behave effectively as scalar fields in the bulk and do not in general contain kinks. Nevertheless, the universal MSS scale will show up, and the morale of this story will be reiterated: it is the scale of near-horizon fluctuations which can appear in various correlation functions.

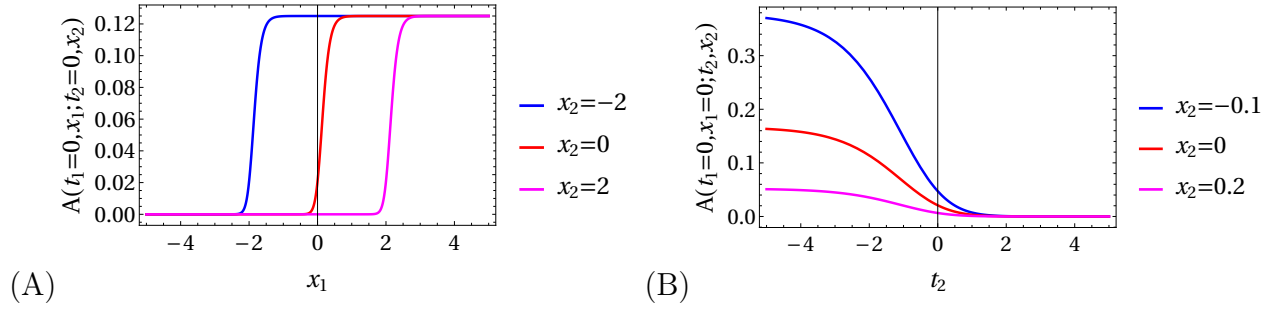


Figure 2.2: Two-point function $G(t_1, x_1; t_2, x_2)$ corresponding to the scattering of an in-falling and an outgoing wave in AdS-Rindler background, at temperature $2\pi T = 1$. In (A) we show the spatial dependence $G(t_1 = 0, x_1, t_2 = 0, x_2)$, in (B) we plot the time dependence $G(t_1 = 0, x_1 = 0, t_2, x_2)$, in both cases at three locations x_2 (blue, red, magenta). The function has the form of a single kink located at $t_2 - t_1 = x_2 - x_1 = 0$. The MSS scale and the kink structure arise as a consequence of shock waves in the bulk, without relation to chaos.

Chapter 3

Static open string in black hole background

We start with the simplest case, that of static open string stretching from the horizon to the boundary of AdS-Schwarzschild (AdSS) background. This is the zero-velocity limit of the celebrated dragging (trailing) string model of [33, 34] and numerous follow-up papers: the dragging string describes a heavy quark moving in a thermal plasma with drift velocity v , thus the static case describes a heavy quark at rest, but in both cases there is the Brownian motion from interactions with the quark-gluon plasma. We use this simple setup also to introduce the general formalism of the near-horizon expansion of variational equations by which we estimate Lyapunov exponent. We will here study the AdSS background in general dimension D ; it is easy enough to do the calculation for any D , and the outcome can be compared with the dynamics of open strings in various D-brane backgrounds – the D1-D5-p black string contains AdS₃, while the stack of D3 branes, the quintessential system for holography, contains the AdS₅ throat.

3.1 AdS Schwarzschild back hole: setup

Throughout the paper we will consider only the bosonic sector of the string. Most of the time we will use the Polyakov action, but sometimes we will switch to the Nambu-Goto action, depending on the problem at hand. Some analytic solutions to the equations of motion are much easier to obtain using the Nambu-Goto action, while the Polyakov action works better with numerics.

3.1.1 Nambu-Goto action

Dynamics of strings in D -dimensional AdS-Schwarzschild spacetime on the Poincare patch with the time coordinate t , radial coordinate r and transverse spatial coordinates x_i , $i = 1, \dots, D - 2$

$$ds^2 \equiv G_{\mu\nu}(x)dx^\mu dx^\nu = r^2 (-h(r)dt^2 + d\vec{x}^2) + \frac{dr^2}{r^2 h(r)}, \quad h(r) = 1 - \left(\frac{r_h}{r}\right)^{(D-1)}, \quad (3.1)$$

can be described by the Nambu-Goto action of the following form

$$S_{\text{NG}} = \frac{1}{2\pi\alpha'} \int d\tau d\sigma \sqrt{-\det \gamma}, \quad (3.2)$$

obtained by constructing an invariant worldsheet volume integral out of an induced metric $\gamma_{\alpha\beta} = G_{\mu\nu}\partial_\alpha X^\mu\partial_\beta X^\nu$ on the worldsheet embedded in spacetime geometry given by (3.1). Here and in the rest of the paper $\alpha, \beta, \dots \in \{\tau, \sigma\}$ and $\mu, \nu, \dots \in \{t, r, \vec{x}\}$ stand for worldsheet and spacetime indices respectively. Latin indices i, j, \dots count the transverse coordinates x_1, \dots, x_{D-2} . A set of scalar fields that live on the string worldsheet $X^\mu = \{t(\tau, \sigma), R(\tau, \sigma), X_i(\tau, \sigma)\}$ are the dynamical variables of the theory. One can easily show that equations of motion are consistent with the static gauge and the ansatz

$$t = \tau, \quad R = \sigma, \quad X_1 = X_1(\tau, \sigma), \quad X_i = 0, \quad i = 2, \dots, D-1. \quad (3.3)$$

This solution represents a fluctuating string stretched from the boundary to the horizon in the $r-x_1$ plane; identifying time and radial coordinate with the worldsheet coordinates τ and σ respectively is known as the static gauge. In [48] it is argued that small fluctuations of X_1 around the straight string solution $X_1 = 0$ encode for chaotic dynamics in field theory, thanks to the existence of a horizon. The argument goes as follows. Consider the worldsheet geometry corresponding to the background (3.1), with the ansatz (3.3) at $X_1 = 0$:

$$ds_{\text{ws}}^2 \equiv \gamma_{\alpha\beta} dX^\alpha dX^\beta = -r^2 f(r) dt^2 + \frac{dr^2}{r^2 f(r)}. \quad (3.4)$$

This is formally a two-dimensional black hole solution with a thermal horizon. Since black holes are known as fast scramblers [1] and maximally chaotic systems [2], any additional stringy fluctuations on top of (3.4) would show some chaotic features *of the dual field theory*. In [48, 49], this is made concrete by computing the worldsheet OTOC which turns out to saturate the chaos bound. But this does not answer our main question: *what is the meaning of bulk chaos?*

3.1.2 Polyakov action

To study the bulk chaos, it is more convenient to abandon the static gauge and use the conformal gauge instead, where the worldsheet metric is diagonal. The easiest way is to write the Polyakov action for the string, solve the constraint and fix the residual gauge freedom by equating the worldsheet metric to the unit matrix. The Polyakov action for the same open string setup in the same AdS-Schwarzschild metric (3.1) reads:

$$S_P = -\frac{1}{2\pi\alpha'} \int d\tau d\sigma \eta^{\alpha\beta} \partial_\alpha X^\mu \partial_\beta X^\nu G_{\mu\nu}(X). \quad (3.5)$$

The dynamics of a planar open string stretching from the horizon at $r = r_h$ to the boundary at $r = \infty$, now imposes the ansatz

$$t = t(\tau), \quad R = R(\sigma), \quad X_1 = X_1(\tau, \sigma), \quad X_j = X_j(\tau), \quad j = 2, \dots, D-2. \quad (3.6)$$

Equations of motion together with the Virasoro constraints read

$$\ddot{t}(\tau) = 0, \quad \ddot{X}_j(\tau) = 0, \quad j = 2, \dots, D-2 \quad (3.7)$$

$$\begin{aligned} & -2h^3(R)R^4(\sigma) - (R(\sigma)h'(R) + 2h(R))R'^2(\sigma) + 2h(R)R(\sigma)R''(\sigma) + \\ & + h^2(R)R^4(\sigma) \left[-R(\sigma)h'(R) + 2 \left(X_1'^2(\tau, \sigma) + \dot{X}_1^2(\tau, \sigma) + \sum_{j=2}^{D-2} \dot{X}_j^2(\tau) \right) \right] = 0, \end{aligned} \quad (3.8)$$

$$2R'(\sigma)X_1'(\tau, \sigma) + R(\sigma) \left(X_1''(\tau, \sigma) - \ddot{X}_1(\tau, \sigma) \right) = 0, \quad (3.9)$$

$$\frac{R'^2(\sigma)}{R^4(\sigma)} + h(R) \left(-h(R)\dot{t}^2(\tau) + X_1'^2(\tau, \sigma) + \dot{X}_1^2(\tau, \sigma) + \sum_{j=2}^{D-2} \dot{X}_j^2(\tau) \right) = 0, \quad (3.10)$$

$$X_1' \cdot \dot{X}_1 = 0. \quad (3.11)$$

The equations for t, X_2, \dots, X_{D-2} (3.7) are trivially satisfied when these are functions linear in τ , thus we can set $t = \tau$ and $X_j = \text{const}$. Moreover, the second constraint (3.11) requires X_1 to depend on one variable only. We choose $X_1 = X_1(\sigma)$ as the more relevant case for us – the static open string/heavy quark.¹ Now the remaining equation for $R(\sigma)$ (Eq. 3.8), together with the nontrivial Virasoro constraint (3.10), also decouples from $X_1(\sigma)$ and simplifies to the following form

$$4h^3(R)R^3(\sigma) + h^2(R)h'(R)R^4(\sigma) + h'(R)R'^2(\sigma) - 2h(R)R''(\sigma) = 0. \quad (3.12)$$

The same equation can be derived from the effective Lagrangian, obtained by first substituting the trivial solutions $t = \tau$ and $X_j = 0, \forall j \neq 1$ into the Polyakov Lagrangian, and then making use of Virasoro constraint (3.10) to eliminate $X_1'^2$:

$$\mathcal{L}_{\text{eff}} = \frac{-h^2(R) - f(R)R'^2(\sigma) - h(R)X_1'^2(\sigma)}{\sqrt{f(R)}h(R)}. \quad (3.13)$$

This Lagrangian describes a static open string stretching from the boundary to the horizon, i.e. the static case of the fluctuating ansätze (3.3,3.6). It has the worldsheet energy as its integral of motion and is thus integrable, as we will argue more rigorously in the following section.

The explicit solution of Eq. (3.12) can only be found numerically. For numerical integration it is better to make a coordinate transformation $r \mapsto 1/r \equiv z$, that will in this context also act as a worldsheet field redefinition. For convenience we will write here the equation of motion also for the Z coordinate obtained simply from plugging $R \mapsto 1/Z$ into Eq. (3.12):

$$4h^3(Z) - h^2(Z)h'(Z)Z(\sigma) - (h'(Z)Z(\sigma) - 4h(Z))Z'^2(\sigma) + 2h(Z)Z(\sigma)Z''(\sigma) = 0, \quad (3.14)$$

where $h(z) = 1 - (z/z_h)^{D-1}$.

For an open string one needs to supply boundary conditions for both endpoints. The physical interpretation of the string as a quark implies that one endpoint has to sit on

¹In Appendix A we show that the opposite case – time-dependent straight string with $X_1 = X_1(\tau)$ – has a trivial dynamics with zero Lyapunov exponent. For a fully general dynamics of $X_1(\tau, \sigma)$ we would need a more general ansatz, leading to a system of partial differential equations. This is beyond the scope of this paper.

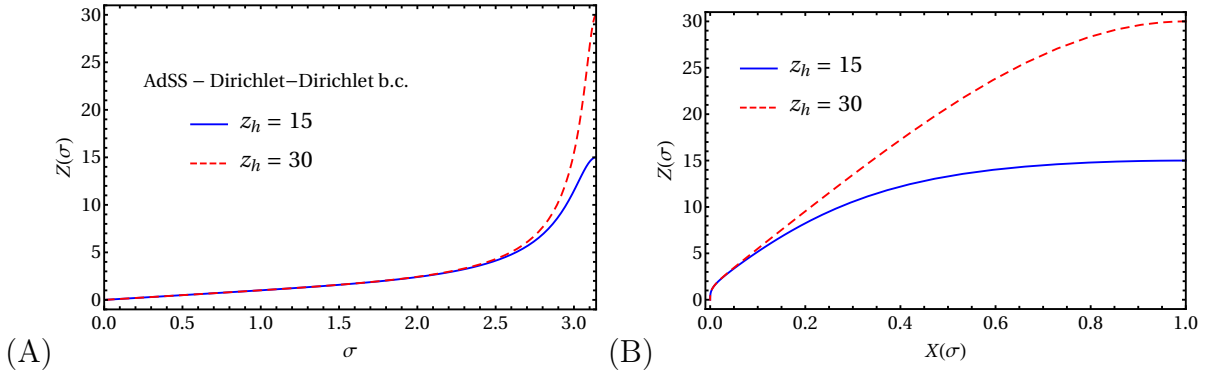


Figure 3.1: Profile of the stationary open string lying in the $z - x_1$ plane of AdS-Schwarzschild geometry, hanging from the boundary $z = 0$ to the horizon $z = z_h$ (we have rescaled the worldsheet coordinate σ so that it goes from 0 to π), obtained by solving numerically Eq. (3.14) with Dirichlet boundary conditions at both ends. We show the radial profile (A) and the shape of the string in the $z - x_1$ plane (B), for the horizon radii $z_h = 15$ (blue) and $z_h = 30$ (red dashed). While extremely simple, this system has nontrivial radial fluctuations.

the boundary [33, 34], therefore we impose the Dirichlet condition on the AdS boundary $Z(\sigma = 0) = 0$. The location of the other end determines the quark mass: a string reaching the horizon describes a "heavy" quark² whereas ending the string on a flavor brane between the boundary and the horizon makes the quark mass finite. For simplicity and also in order to explore the near-horizon dynamics, we opt for the first option and fix the other end at $Z(\sigma = \pi) = z_h$, solving the equation with Dirichlet boundary condition at both ends.³

Finally, one word of caution is in order. Looking at the static gauge ansatz (3.3), one might worry that the radial profile $R(\sigma)$ and its variation $\delta R(\sigma)$ are parametrization-dependent, i.e. correspond to changing the gauge from $R = \sigma$ to some nontrivial function $R(\sigma)$. This is not true, as the parametrization invariance is partially fixed by imposing the conformal gauge, and the residual invariance is fixed by imposing the flat worldsheet metric and the boundary condition for the transverse coordinate X_1 . Therefore, in this setup, the radial dynamics is physical; had we not fixed the boundary conditions, the same physics would be encoded in the residual parametrization invariance as in [49].

At this point we give the basic information on the numerics. Here and in further numerical work, we solve the two-point boundary value problem for the string using the collocation pseudospectral algorithm originally developed in [50]. Alternatively, it is possible to use the built-in NDSolve routine in Wolfram Mathematica, however in most cases this does not work so well. The same method is used for the variational equations.

3.2 Integrability in AdS-Schwarzschild

Let us now prove that the motion of an open string in AdS-Schwarzschild background is integrable, unlike the motion of closed string which is nonintegrable in the presence

²The quark is heavy in the sense that its mass is much larger than all other energy scales in the problem.

³The range of the σ coordinate depends on the parametrization, we keep the textbook range $0 \leq \sigma < \pi$ just for convenience.

of a black hole [51, 52]. We will perform the same type of analysis that is done in [51], exploiting the Kovacic algorithm [53, 54, 55, 51, 56]. The algorithm can be described as follows:

1. Find an integrable solution to the equations of motion. This solution will represent one member of a class of solutions differing only by first integrals (i.e., conserved quantities); the whole class forms an invariant (hyper)plane of solutions.
2. Write down the equation of motion for a variation normal to the previously described invariant plane of solutions, the so-called normal variational equation (NVE).
3. Solve the NVE so obtained and check whether it is expressible in terms of Liouvillian functions. These are the elementary functions (powers, exponentials, trigonometric functions and their inverses), rational functions of such elementary functions, and their integrals. The existence of such a solution is equivalent to the solvability of the identity component G^0 of the Galois group; conversely, their nonexistence is equivalent to G^0 being not solvable, and hence non-Abelian. Non-Abelian nature of G^0 tells us that no complete system of integrals of motion in involution exists, therefore the system is nonintegrable.

We want to show the integrability of the system described by the effective Lagrangian given by Eq. (3.13). One obvious invariant plane is the $R - X_1$ plane for a straight string solution:

$$R(\sigma) = r_h, \quad X_1(\sigma) = \text{const.} \equiv X_c. \quad (3.15)$$

One can see that this plane is invariant simply by observing that the canonical momentum corresponding to the off-plane motion is zero: $p'_X = \partial\mathcal{L}_{\text{eff}}/\partial X_1 = 0$. The corresponding normal variational equation along the X_1 -direction is trivial: $\delta X_1'' = 0$, yielding the conclusion that the system is integrable. In the next section we will see that despite being integrable, this system exhibits an exponential growth of the in-plane variation with a positive Lyapunov-like exponent in the near-horizon region. This is likely a consequence of the near-horizon symmetries of non-extremal black holes, as argued in [42, 43] and elaborated in Appendix B. By itself this is not surprising: a local instability can always lead to a growing mode even in a trivially integrable system, the simplest example being the inverse chaotic oscillator [57]. This is similar to findings of [26] where it is noted that horizons are really a nest of chaos in holography. Namely, even integrable systems can display local instability in the vicinity of thermal horizons.

We need to make one thing clear. The integrability of the static open string Lagrangian (3.13) that we have demonstrated in no way conflicts the established nonintegrability of string motion in black hole and D-brane backgrounds proved in [51, 55]. The fact that a ring string in these backgrounds is nonintegrable, as found in the aforementioned references, is enough to prove the nonintegrability of string motion in these geometries in general. On the other hand, the existence of special solutions and boundary conditions which are integrable (and therefore nonchaotic) is perfectly expected also in a nonintegrable system.

3.3 Lyapunov exponent near the AdS-Schwarzschild horizon

Instead of calculating the out-of-time-ordered correlators that are typically used in the literature to calculate the Lyapunov exponent in field theory, either with a gravity dual in which case it can be done holographically, or through the usual field-theoretical perturbation theory by summing the ladder diagrams, here we exploit a much simpler technique, motivated by the one used in [21, 23, 26], and appropriate for the study of bulk chaos. We want to know whether we can learn something about the field theory side by studying classical fluctuations around some stringy solutions in the bulk. Something similar is done in the study of pole-skipping of the metric fluctuations [58] where the special points in the energy-momentum plane for the metric fluctuations determine the OTOC, a *four-point* function. We will find that the variation of worldsheet string solutions (with given start- and endpoint) can tell us about off-equilibrium two-point correlation functions in dual CFT.

Studying *spatial* dependence of the worldsheet field, i.e. the function $R(\sigma)$ and calling it dynamics as we do might be controversial; so is the term Lyapunov exponent for the growth exponent of the variation $\delta R(\sigma)$. The important difference between σ and τ dynamics is that the worldsheet time is unbounded and one can define asymptotic quantities as is usually done for the Lyapunov exponent (defining it as the limit of small initial variation and long-time evolution $\lambda = \lim_{t \rightarrow \infty} \lim_{\delta x(0) \rightarrow 0} \log(\delta x(t))/t$, for some generic coordinate x). The extent of the σ coordinate is finite and there is no analogue to $\lim_t \rightarrow \infty$. Therefore, while we talk all the time of Lyapunov exponents, we really study what is often called finite-time Lyapunov indicator in the context of time evolution, i.e. the exponent defined locally rather than asymptotically. This is however often assumed as a matter of course: the bulk Lyapunov exponent (in time) computed, e.g. in [21, 23, 59], is also the finite-time quantity.

For solving the variational equations it is convenient to go again for the Polyakov action in the conformal gauge. The ansatz for the static open string is the same as in Eq. (3.6). Here we are particularly interested in studying the variation near the horizon. To that end, we substitute $R(\sigma) \mapsto r_h + \varepsilon \delta R(\sigma)$ into Eq. (3.12) and expand it in ε small to linear order. This yields the near-horizon variational equation:

$$\delta R'' - (D-1)^2 r_h^2 \delta R = 0. \quad (3.16)$$

The solution is thus $\delta R \propto e^{\pm 2\lambda_L \sigma}$ with a pair of Lyapunov exponents of equal magnitude and with opposite signs, as it has to happen in a Hamiltonian system. The exponent saturates the Maldacena-Stanford-Shenker (MSS) bound [2]:

$$\lambda_L = \frac{(D-1)r_h}{2} = 2\pi T. \quad (3.17)$$

The reason why we define the Lyapunov exponent with a factor of 2, i.e. through $\delta R \propto e^{\pm 2\lambda_L \sigma}$ instead of $\delta R \propto e^{\pm \lambda_L \sigma}$ is that the same expression appears also in the OTOC growth, and follows from the definition of OTOC on the thermal circle. Here, for bulk equations of motion, this argument is irrelevant but we nevertheless want to stay consistent with the definition of the MSS bound as we want to compare and relate the two situations.

We have shown that the MSS bound is saturated regardless of the spacetime dimension or any other parameters save the temperature. While it is tempting to call this "maximal

chaos in the bulk", we already know from our integrability analysis that this system is not chaotic at all. How then should we interpret the result? Since our system is not chaotic, we are left with the conclusion that we have actually encountered some sort of unstable saddle point in our system. Therefore we should interpret λ_L not as Lyapunov exponent *in dual field theory*, but as some characteristic scale that will likely correspond to relaxation time of some perturbations around a thermal horizon.

3.4 Lyapunov exponent near a general hyperscaling-violating horizon

In order to further corroborate the universality of the result (3.17), we closely follow the idea of [26] and study bulk motion in a broad class of bulk geometries: hyperscaling-violating horizons at finite temperature, constructed in [60, 61, 62, 63] as gravity duals of effective field-theories with scaling and long-range entanglement, thought to be ubiquitous in quantum-many body systems. In [26], it is shown the bulk geodesics, i.e. particle orbits also have the MSS value of the Lyapunov exponent in a broad part of the parameter space (though not everywhere); here we show that static strings/holographic heavy quarks *always* have the MSS value. The background metric reads

$$ds^2 = -r^{2\zeta - \frac{2\theta}{D-2}} f(r) dt^2 + \frac{1}{f(r)r^{2 + \frac{2\theta}{D-2}}} dr^2 + r^2 d\vec{x}^2, \quad f(r) = 1 - \left(\frac{r_h}{r}\right)^{D-2+\zeta-\theta}, \quad (3.18)$$

and depends on two parameters, the Lifshitz exponent ζ that measures the anisotropy of space versus time scaling (so that Lorentz-invariant backgrounds correspond to $\zeta = 1$) and the hyperscaling exponent θ which measures the deviation from the dimensional scaling of free energy and roughly corresponds to long-range-entangled degrees of freedom. By definition, the temperature of the horizon at r_h is found as:

$$4\pi T = -\frac{g'_{tt}(r_h)}{\sqrt{g_{tt}(r_h)g_{rr}(r_h)}} = (D - 2 - \theta + \zeta)r_h^\zeta. \quad (3.19)$$

We can easily redo the same analysis as for the AdSS configuration, keeping the same ansatz (3.6) and the equations of motion analogous to (3.7-3.11). When everything is said and done, we obtain the near-horizon variational equation

$$\delta R''(\sigma) - (D - 2 - \theta + \zeta)^2 r_h^{2\zeta} \delta R(\sigma) = 0, \quad (3.20)$$

which, according to (3.19), implies again $\lambda_L = 2\pi T$ with the ansatz $\delta R \sim \exp(2\lambda_L \sigma)$.

Finally, while one might naturally be interested also in the dynamics of transverse coordinates such as $X_1(\tau, \sigma)$,⁴ we have already mentioned (after the equations of motion (3.7-5.10) and in Appendix A) that time-dependent fluctuations are always linear and thus irrelevant for the study of bulk instabilities (let alone chaos).⁵

⁴In most applications related to holographic heavy quarks, it is precisely the dynamics of X_i coordinates that describes drift, diffusion and other relevant phenomena, such as in pioneering works [33, 34] and later developments [64]; the field-theory correlation functions are determined by the near-boundary behavior of the transverse fluctuations.

⁵As a side note, a special *exact* solution of the equations of motion is a string lying on the horizon, i.e. with nontrivial profile $X_1(\sigma)$ but with $R(\sigma) = r_h$. In this case, the variational equation (3.16) also becomes exact on the whole worldsheet, yielding again $\lambda_L = 2\pi T$ as in Eq. (3.17). Such a solution is however difficult to interpret holographically so we do not study it further.

Chapter 4

Intermezzo: Static open string in black brane backgrounds

In this chapter we generalize the findings for the AdS black hole backgrounds to black brane geometries. These geometries arise generically as semiclassical supergravity solutions at finite temperature. Indeed, AdS black holes typically appear as near-brane expansions of these more general solutions. Although the full brane geometries typically have flat asymptotics and thus do not have a holographic dual, they serve a double purpose in our work. First, they will provide additional evidence that a thermal horizon is the source of local instability leading to the MSS Lyapunov exponent, no matter what the far-from-horizon physics is. Second, considering the leading deformation away from AdS geometry in the near-brane region corresponds to a Coulomb deformation in dual CFT [29]. Therefore, the black brane calculation can actually serve as the starting point in exploring the dynamics of a heavy quark in a Coulomb-deformed plasma.

To the best of our knowledge no systematic work was done on string dynamics in brane backgrounds, except for the general proofs of nonintegrability in [51, 55]. A black brane setup was considered in [33] but with different field content and metric than in our case (they consider D7 branes while we consider D3 branes).

4.1 Extremal black D3 brane

Consider first the extremal black brane geometry made out of a stack of Q coincident D3-branes. This is a well-known stringy analog of an extremal charged black hole in Einstein-Maxwell theory, which develops an infinite throat interpolating between flat space at infinity and $\text{AdS}_2 \times \mathbb{S}^2$ near-horizon region. Equivalently, extremal black brane can be thought of as interpolating between the ten-dimensional Minkowski spacetime and $\text{AdS}_5 \times \mathbb{S}^5$ space. In this context it is the embedding of the textbook holographic theory, the classical supergravity on $\text{AdS}_5 \times \mathbb{S}^5$ [40]. The metric reads

$$ds^2 = \frac{\eta_{\mu\nu} dx^\mu dx^\nu}{f^2(r)} + f^2(r) (dr^2 + r^2 d\Omega_k), \quad \mu = 0, \dots, n-1 \quad (4.1)$$

$$f(r) = \left(1 + \frac{Q}{r^n}\right)^m, \quad n = 4, m = \frac{1}{4}, k = 5. \quad (4.2)$$

Here, r is the radial coordinate, x^μ are the directions on the brane, while $d\Omega_k$ is the k -sphere with coordinates Φ_1, \dots, Φ_k . The string configuration we consider is completely

analogous to the static open string studied previously in AdS black hole backgrounds:

$$\begin{aligned} t &= t(\tau), & X_1 &= x_1, & X_2 &= x_2, & X_3 &= x_3, \\ R &= R(\sigma), & \Phi_1 &= \Phi_1(\tau), & \Phi^2 &= \Phi_2(\tau), & \Phi_3 &= \phi_3, & \Phi_4 &= \phi_4, & \Phi_5 &= \phi_5 \end{aligned} \quad (4.3)$$

The equation of motion for T requires $\dot{t}(\tau) = 0$ so we choose a gauge in which $t(\tau) = v\tau$. We have one nontrivial Virasoro constraint and an additional constraint coming from the above ansatz, i.e. the assumption that R only depends on σ :

$$\dot{\Phi}_1^2 + \sin \Phi_1^2 \dot{\Phi}_2^2 \equiv \ell^2, \quad (4.4)$$

where ℓ^2 is the conserved squared angular momentum on the 5-sphere. The constraints decouple the dynamics of R from Φ^1 and Φ^2 :

$$R'' - \frac{R'^2}{R} + v^2 \frac{1 + 2Rf'/f}{f^4 R} = 0 \quad (4.5)$$

$$\ddot{\Phi}_1 + \left(\dot{\Phi}_1^2 - w^2 \right) \cot \Phi_1 = 0. \quad (4.6)$$

We have some analytical control over the above equations in two opposite limits, for small R where we recover the $\text{AdS}_5 \times \mathbb{S}^5$ throat, and for large R , in the flat space limit.¹ These cases are both integrable, as shown in [51]. The question is thus what happens with integrability for some generic value of Q . Again [51] provides the general answer: string motion at finite Q is nonintegrable. But we have seen in the AdS black hole case that a static open string can live in an integrable sector. We thus check the integrability of our ansatz (4.3) with the Kovacic algorithm. The result is that this system is integrable, just like in the AdSS background, due to the relatively simple form of the string configuration (4.3).

Finding the explicit solution for $R(\sigma)$ and $\Phi_1(\sigma)$ in terms of elementary functions is a hopeless task. However, this is not necessary, as we mainly want to analyze the variational equations in the near-horizon limit. The radial variational equation reads

$$\delta R'' - \frac{2R'}{R} \delta R' + 2v^2 \left(\frac{R'^2}{2R^2} + \frac{Rf'' - 2f'}{f^5 R} - \frac{1}{2f^4 R^2} - \frac{5f'^2}{f^6} \right) \delta R = 0, \quad (4.7)$$

and just like the on-shell equations it is also tractable in the two extremal cases: in the AdS throat and in the far (flat-space) region. In the former case, (4.7) becomes

$$\delta R'' - (3\epsilon^2 v^2 / Q) \delta R = 0, \quad (4.8)$$

where $R \sim \epsilon$, i.e. the small parameter is the distance from the brane; since this limit means $\epsilon \rightarrow 0$, the bulk Lyapunov exponent vanishes. In the flat-space limit we obtain $\delta R'' - \epsilon^2 v^2 \delta R = 0$, where now $R \sim 1/\epsilon$, so again the Lyapunov exponent vanishes. There is no instability at zero temperature. We will see the opposite situation with black D-branes, in the presence of a thermal horizon.

¹Alternatively one can think of these two limits as $Q \rightarrow \infty$ and $Q \rightarrow 0$.

4.2 Non-extremal black D3 brane

We will now consider a non-extremal black brane, the finite-temperature generalization of the extremal solution at temperature T :

$$ds^2 = -h(r) \frac{dt^2}{f^2(r)} + \frac{d\vec{x}^2}{f(r)^2} + f^2(r) \left(\frac{dr^2}{h(r)} + r^2 d\Omega_k^2 \right) \quad (4.9)$$

$$f(r) = \left(1 + \frac{Q}{r^n} \right)^m, \quad h(r) = 1 - \left(\frac{r_h}{r} \right)^4, \quad n = 4, m = \frac{1}{4}, k = 5 \quad (4.10)$$

$$\frac{1}{T} = \frac{4\pi f(r_h)}{\sqrt{h'(r_h)(h(r)/f^2(r))'|_{r=r_h}}} = \frac{\pi \sqrt{Q + r_h^4}}{r_h}. \quad (4.11)$$

In the limit $r_h \rightarrow 0$ (equivalently, $T = 0$) the black brane becomes the previously studied extremal black brane. The coordinates are the same as in the extremal solution (4.2). The $d\Omega_5$ sector is insensitive to temperature, which can be seen from the fact that its metric is independent of the redshift function h . The effect of the thermal horizon is thus seen solely in the equation of motion for R :

$$h(R)R(\sigma)R''(\sigma) + h(R)R(\sigma) \left(\frac{f'(R)}{f(R)} - \frac{h'(R)}{2h(R)} \right) R'^2(\sigma) + \frac{v^2 h^3(R)R(\sigma)}{f^4(R)} \left(\frac{f'(R)}{f(R)} - \frac{h'(R)}{2h(R)} \right) - \frac{\ell^2 h^2(R)R^2(\sigma)}{f^4(R)} \left(1 + R(\sigma) \frac{f'(R)}{f(R)} \right) = 0, \quad (4.12)$$

where ℓ^2 has the same meaning as in Eq. (4.4). The system again has two independent degrees of freedom, one of which, the radial coordinate $R(\sigma)$, exhibits integrable dynamics at $T = 0$, as we have shown explicitly through the Kovacic algorithm, and presumably at $T \neq 0$.

We can use nontrivial Virasoro constraint

$$f^2(R) \left(\frac{R'^2(\sigma)}{h(R)} - \ell^2 R^2(\sigma) \right) - \frac{v^2 h(R)}{f^2(R)} = 0 \quad (4.13)$$

to eliminate ℓ^2 from the equation (4.12), yielding

$$2h(R)R(\sigma)R''(\sigma) - (2h(R) + R(\sigma)h'(R))R'^2(\sigma) + \frac{2v^2 h^3(R)}{f^4(R)} \left(1 - R(\sigma) \left(\frac{h'(R)}{2h(R)} + 2 \frac{f'(R)}{f(R)} \right) \right) = 0. \quad (4.14)$$

Following the same logic as before, we find the near-horizon variational equation:

$$\delta R'' - \frac{16r_h^2}{Q + r_h^4} \delta R = 0 \quad (4.15)$$

Looking for a solution of a form $\sim \exp(2\lambda_L \sigma)$ and using Eq. (4.11), we find that $\lambda_L = 2\pi T$. The ubiquitous MSS bound is present even in a non-holographic geometry, again in the context of integrable dynamics with an unstable saddle point. We thus strengthen the important realization from the previous chapter and [26]: thermal horizons are the generators of instability, not necessarily chaos. The holographic meaning of this instability is theory-dependent, and may not exist when there is no AdS asymptotics.

4.3 Numerical solutions

In this section we solve the equations of motion numerically as this is the only way to obtain a look at the string in the whole space. We will see explicitly that the dynamics is integrable and yet that the variational equations have exponentially growing solutions.

The aim is to solve Eq. (4.14) and its variational equation. In order to do so, it is more convenient to use the coordinates $z = 1/r$, so that the relevant equation now becomes

$$Z'' - \frac{Z'^2}{Z} - \frac{h'(Z)Z'^2}{2h(Z)} - \frac{v^2 h^2(Z)Z^3}{f^4(Z)} \left(1 - Z \left(\frac{2f'(Z)}{f(Z)} + \frac{h'(Z)}{2h(Z)} \right) \right) = 0. \quad (4.16)$$

We impose Dirichlet conditions at the brane and Neumann conditions at the other end (open strings should be attached to branes but they can float freely in the asymptotically flat outer region). Once we have the solutions $R(\sigma)$ we can use that solution to solve also the variational equation:

$$\begin{aligned} \delta Z'' - \frac{(2h(Z) + Zh'(Z))Z'}{Zh(Z)} \delta Z' + \frac{1}{2Z^2} & \left[\frac{Z'^2(2h^2(Z) + Z^2h'^2(Z) - h(Z)Z^2h''(Z))}{h^2(Z)} \right. \\ - \frac{20v^2h^2(Z)Z^6f'^2(Z)}{f^6(Z)} + \frac{4v^2h(Z)Z^5(3f'(Z)(2h(Z) + Zh'(Z)) + h(Z)Zf''(Z))}{f^5(Z)} \\ & \left. - \frac{v^2Z^4(6h^2(Z) + Z^2h'^2(Z) + h(Z)Z(8h'(Z) + Zh''(Z)))}{f^4(Z)} \right] \delta Z = 0. \quad (4.17) \end{aligned}$$

For δZ the meaningful boundary condition is the fixed (and small) difference between the on-shell trajectory and its clone at the brane ($\delta Z(\sigma = 0) = \epsilon$) and the Neumann condition at infinity (since the strings float freely so does the difference between to string profiles). The outcome is given in Fig. 4.1. Along with the radial profiles of the string for different temperatures, we plot the near-horizon values of the numerically computed Lyapunov exponent $\lambda_L^{(n)} = \log(\delta Z(\sigma_0)/\epsilon)/2$, where σ_0 is some near-brane cutoff (we want the Lyapunov exponent near the brane thus σ_0 should cut off the far-from-brane part).² The numerics is reasonably close to the MSS result, providing an additional confirmation.

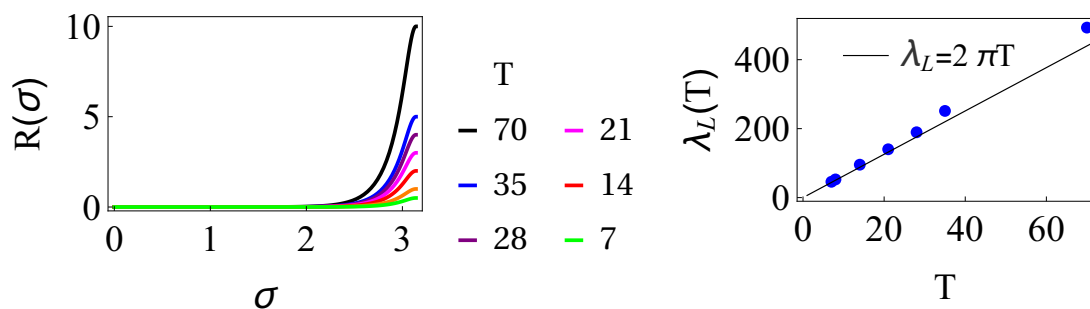


Figure 4.1: Radial profile $Z(\sigma)$ (A) and the numerical Lyapunov exponent $\lambda_L^{(n)} = \log(\delta Z(\sigma_0)/\epsilon)/2$ (B) for the static open string in thermal black brane background, for a range of temperatures T . We take $\sigma_0 = 0.2$ for the cutoff but values between 0.1 and 0.5 yield similar results. We compare the numerical result for the Lyapunov exponents to the analytic estimate (i.e., the chaos bound) and find reasonable agreement.

²Of course, one needs to check that the results do not strongly depend on σ_0 .

Chapter 5

Open string in D1-D5-p black string background

5.1 Introduction

So far we have explored the bulk instability of open strings in black hole and black brane backgrounds and we have found the saturation of the MSS bound, clearly unrelated to chaos as the system is integrable. Now we will interpret this finding and relate it to the thermalization rate and thermal correlators in a theory which is particularly interesting as we know something not only about the (super)gravity solution and the corresponding large- N field theory, but also about the microscopics: the D1-D5-p black string [65, 66, 67, 40, 41]. This setup is celebrated also for being the first black hole solution in string theory for which the entropy was computed by counting the microscopic degrees of freedom, obtaining for a horizon area A the semiclassical Bekenstein-Hawking result $S = A/4$ [66]. Another famous result is the calculation of the greybody factor in [65], the logical macroscopic extension of the entropy calculation. The idea is that the Hawking radiation, emitted by the horizon with perfect blackbody spectrum, is itself scattered by the black hole, therefore an asymptotic observer will measure a different spectrum; the ratio between the two spectra (the asymptotically measured one to the blackbody spectrum) at given energy and angular momentum is called the greybody factor. It is easy to see from [65] that the greybody factor is obtained as the absorption cross section for a wavepacket in the black hole background. In holographic setups, where the relevant near-horizon dynamics is dual to a two-dimensional CFT, the absorption cross section can be obtained from the imaginary part of the retarded Green's function.

Our idea here is twofold. First, we will study the Lyapunov stability in D1-D5-p background – this may (and will) yield some surprises as the geometry has a global rotation with angular velocity Ω . So far we have only studied static geometries and it is not obvious whether the conclusions carry over to the rotating case. Second and more important, we will relate the Lyapunov exponent to the retarded propagator in dual field theory and pinpoint what it tells us about the microscopic meaning of bulk instability.

5.2 Setup

The background describing the D1-D5-p black string reads

$$ds^2 = \frac{1}{\sqrt{f(r)}} \left(-dt^2 + dx_5^2 + \frac{r_0^2}{r^2} (\cosh \Sigma dt + \sinh \Sigma dx_5)^2 \right) + \sqrt{f(r)} \left(\frac{dr^2}{h(r)} + r^2 (d\psi^2 + \sin^2 \psi (d\theta^2 + \sin^2 \theta d\phi^2)) \right), \quad (5.1)$$

$$f(r) = \left(1 + \frac{r_1^2}{r^2} \right) \left(1 + \frac{r_5^2}{r^2} \right), \quad h(r) = 1 - \frac{r_0^2}{r^2}. \quad (5.2)$$

Here, t and r are the time and radial coordinate respectively, ψ , θ and ϕ are the angles on a 3-sphere, and x_i ($i = 1, \dots, 5$) are the Cartesian coordinates in the plane. This is a classical solution of ten-dimensional type IIB supergravity compactified on $T^5 \cong T^4 \times \mathbb{S}^1$ [65, 41]. It is charged under the Ramond-Ramond field of the corresponding theory; since D1 and D5 branes are magnetically dual to each other we get electric and magnetic charges that are related to the radii r_1 and r_5 , respectively. One can think of these charges also as representing the number of copies in the stack of D1 branes compactified on \mathbb{S}^1 along the x_5 direction, and in the stack of D5 branes wrapping the whole $T^4 \times \mathbb{S}^1$ manifold. There is also an additional charge associated to the p -momentum along D1-brane, i.e. the Kaluza-Klein (KK) mode on \mathbb{S}^1 , related to factors of $r_0^2 \cosh^2 \Sigma$ in the metric (5.1-5.2). One also notices that this solution is anisotropic and rotating for $\Sigma \neq 0$ due to the presence of non-vanishing tx_5 -component in the metric tensor (5.1). The temperature and entropy are given by

$$\frac{1}{T} = \frac{2\pi r_1 r_5 \cosh \Sigma}{r_0}, \quad S = \frac{2\pi^2 r_1 r_5 r_0 \cosh \Sigma}{4}. \quad (5.3)$$

We now remind the reader on some interesting features of this solution. The first is that in the extremal case ($T, S \propto r_0 = 0$), also known as the extremal D1-D5 bound state system, the near-horizon geometry becomes $\text{AdS}_3 \times \mathbb{S}^3$. We can show this by performing the coordinate transformation $t \rightarrow t/\varepsilon L$, $r \rightarrow \varepsilon L r$, $x_5 \rightarrow x_5/\varepsilon L$ in the metric (5.1), where $L^2 = r_1 r_5$: in the limit $\varepsilon \rightarrow 0$ we recover the $\text{AdS}_3 \times \mathbb{S}^3$ geometry

$$ds_{\text{NHE}}^2 \approx \frac{r^2}{L^2} (-dt^2 + dx_5^2) + L^2 \frac{dr^2}{r^2} + L^2 d\Omega_3^2. \quad (5.4)$$

On the other hand in the near-extremal case ($r_0 \rightarrow 0$, $\Sigma \rightarrow \infty$), the p -momentum survives and we still have the full D1-D5-p system, with a near-horizon geometry of the rotating Banados-Teitelboim-Zanelli (BTZ) black hole:

$$ds_{\text{NHNE}}^2 \approx \frac{r^2}{L^2} (-dt^2 + dx_5^2) + L^2 \frac{dr^2}{r^2 - r_0^2} + \frac{r_0^2}{L^2} (\cosh \Sigma dt + \sinh \Sigma dx_5)^2 + L^2 d\Omega_3^2. \quad (5.5)$$

The procedure to derive this is the same as in the extremal black string case, except that now we also need to take $r_0 \rightarrow \varepsilon L r_0$. In order to translate the metric (5.5) into the standard coordinates for BTZ black holes we have to perform an additional coordinate transformation:

$$r^2 = w^2 - w_-^2, \quad w_+ = r_0 \cosh \Sigma, \quad w_- = r_0 \sinh \Sigma. \quad (5.6)$$

For convenience we will write down the metric of rotating BTZ in these coordinates:

$$ds_{\text{BTZ}}^2 = -\frac{(w^2 - w_+^2)(w^2 - w_-^2)}{L^2 w^2} dt^2 + \frac{L^2 w^2 dw^2}{(w^2 - w_+^2)(w^2 - w_-^2)} + \frac{w^2}{L^2} \left(\frac{w_+ w_-}{w^2} dt + dx_5 \right)^2. \quad (5.7)$$

The angular velocity is given by $\Omega = w_-/Lw_+ = \tanh \Sigma/L$. Here we can use the Brown-York tensor for AdS gravity [68] to calculate conserved charges. This is done in Appendix C where we have derived the energy and angular momentum of this black hole solution:¹

$$E = \frac{w_+^2 + w_-^2}{8L^2}, \quad J = \frac{w_+ w_-}{4L^2}. \quad (5.8)$$

We should note that our terminology on what is extremal or near-extremal black string is governed by r_0 and Σ parameters, despite the fact that *in both limits we get extremal D1-D5 and extremal D1-D5-p states, respectively*, i.e. the states which preserve a certain number of supersymmetry generators and are thus Bogomolny-Prasad-Sommerfield (BPS) states that saturate a BPS bound [41]. One crucial difference between the two arising from the additional KK momentum in D1-D5-p is that it has nonzero horizon area and entropy, while also being extremal in the sense that it saturates a BPS bound. This particular feature was exploited in [66] to derive the Bekenstein-Hawking area law by counting the degeneracy of BPS states. On the other hand, the extremal D1-D5 bound state was used in the celebrated Maldacena's paper [67] to conjecture the AdS₃/CFT₂ correspondence.

We can contrast this solution with a more familiar charged black hole solution in Einstein-Maxwell theory, namely the Reissner-Nordström (RN) geometry. An extremal RN solution also saturates the BPS bound due the fact that Einstein-Maxwell theory can be embedded into supergravity theories [69].² Furthermore, in the near-horizon limit of a non-extremal RN we encounter Rindler \times S², while in the extremal case the near-horizon geometry becomes AdS₂ \times S², also known as the Robinson-Bertotti geometry. It is a well known fact that AdS spaces are unstable under small perturbations [70]. We can imagine throwing neutrally charged matter into an extremal RN black hole that would make it slightly non-extremal and therefore would produce such a huge gravitational backreaction that near-horizon geometry would transition from AdS₂ to Rindler space, spoiling AdS asymptotics. On the other hand, if we consider an extremal black string, adding a quantum of momentum p along the D1 direction would result in the transition from AdS₃ to BTZ black hole.

This simple analysis leads us to an important prediction: *we should expect a vanishing Lyapunov exponent in the extremal black string geometry, but a non-vanishing one away from extremality*. The logic is that any growing mode (i.e., a variation with a positive Lyapunov exponent) would destroy the extremal background, hence the growth rate has to be zero; but no such constraint exists away from extremality.

¹It is worth mentioning that when $\Sigma = 0$ from (5.6) we also get $w_- = 0$, which gives vanishing angular momentum $J = 0$ in Eq. (5.8). We see that in the non-rotating limit the BTZ black hole in the near-horizon region has zero angular momentum.

²One should think of both the near-extremal D1-D5 bound state and the extremal D1-D5-p state as higher-dimensional multi-charge versions of the extremal RN solution, while the non-extremal analogue is given by a generic D1-D5-p black string geometry (5.1-5.2).

5.3 Analytic estimate of the Lyapunov exponent

Now we return to our old setup and consider an open string in this background. In particular we postulate the following string configuration

$$\begin{aligned} t(\tau, \sigma) &= v\tau, & R(\tau, \sigma) &\equiv R(\sigma), \\ \Psi(\tau, \sigma) &\equiv \psi(\tau), & \Theta(\tau, \sigma) &\equiv \pi/2, & \Phi(\tau, \sigma) &\equiv \phi(\tau), & X_5(\tau, \sigma) &\equiv X_5(\sigma). \end{aligned} \quad (5.9)$$

All the τ -dependent transversal degrees of freedom $\{\Psi, \Theta, \Phi\}$ decouple, as in all other cases studied in this paper. The remaining fields R and X_5 also decouple from each other, since we can combine the equation of motion for $R(\sigma)$ with the nontrivial Virasoro constraint

$$-v^2 + \frac{f(R)R'^2(\sigma)}{h(R)} + X_5'^2(\sigma) + \frac{r_0^2(v^2 \cosh^2 \Sigma + \sinh^2 \Sigma X_5'^2(\sigma))}{R^2(\sigma)} = 0 \quad (5.10)$$

to obtain the following equation

$$\begin{aligned} 2v^2 f h^2 (-2r_0^2 \cosh^2 \Sigma + R^2) + v^2 f' h^2 R (-r_0^2 \cosh^2 \Sigma + R^2) \\ + f^2 R^2 \left(-(2h + Rh') R'^2 + 2hRR'' \right) = 0. \end{aligned} \quad (5.11)$$

The effective Lagrangian for the coordinates R and X_5 takes the form

$$\mathcal{L} = \frac{1}{\sqrt{f(R)}} \left(v^2 \left(-1 + \frac{r_0^2 \cosh^2 \Sigma}{R^2} \right) - \frac{f(R)R'^2}{h(R)} - \left(1 + \frac{r_0^2 \sinh^2 \Sigma}{R^2} \right) X_5'^2 \right), \quad (5.12)$$

and reproduces Eq. (5.11) when combined with the Virasoro constraint (5.10).

We will assume that we are in the dilute gas regime, like in [65], defined by $r_0, r_0 \cosh \Sigma \ll r_1, r_5$. This boils down to the condition $T \ll 1/r_1, 1/r_5$. We are particularly interested to get an analytic solution to the variational equation of (5.11) in two distinct regions: (i) near-horizon region $r \sim r_0, r_0 \cosh \Sigma \ll r_1, r_5$ and (ii) far region $r_0, r_0 \cosh \Sigma \ll r \sim r_1, r_5$.

Expectedly, the system described by the Lagrangian (5.12) is integrable. Applying again the normal variational equation methods, we can choose the invariant plane to be $\{t = \tau, R = r_0, \Psi = 0, \Theta = \pi/2, \Phi = 0, X_5 = \text{const.}\}$. Since X_5 is a cyclic coordinate in (5.12), its conjugate momentum is constant: $p'_{X_5} = \partial \mathcal{L} / \partial X_5 = 0$. Therefore, the $R - X_5$ plane is indeed invariant under the evolution of the system (along σ). The normal variational equation therefore corresponds to the variations in the X_5 -direction, yielding $\delta X_5'' = 0$. Just like the open string dynamics in AdS-Schwarzschild spacetime, this system is integrable. In both cases, the extra integrals of motion are simply the transverse momenta.

5.3.1 Near-horizon limit

We first solve the variational equation of the radial coordinate in (5.11) obtained by perturbing the horizon solution $R(\sigma) = r_0, R \sim r_0 + \delta R(\sigma)$:³

$$\delta R'' - \frac{\delta R'^2}{2\delta R} - \frac{v^2 \alpha^4}{r_0^6 f^2(r_0)} \delta R = 0, \quad (5.13)$$

$$\alpha^4 \equiv r_0^2(r_1^2 + r_5^2) + 2r_1^2 r_5^2 + r_0^2(2r_0^2 + r_1^2 + r_5^2) \cosh(2\Sigma) \quad (5.14)$$

³One would expect that a variational equation should be linear, but we here encounter non-linear one. This is due the fact that Eq. (5.11) contains redshift function $h(r)$ in front of every term, so that upon expanding around r_0 linear terms would vanish since $h(r_0) = 0$.

It is possible to find an analytic solution, which depends on the parameter C (determined by the initial conditions):

$$\delta R(\sigma) = \cosh^2 \left(\frac{v\sqrt{\mathfrak{a}^4}(-\sigma + 2Cr_0^6 f^2(r_0))}{\sqrt{2r_0^3}f(r_0)} \right) \quad (5.15)$$

We are interested in the asymptotic growth of the solution $\sim e^{2\lambda_L\sigma}$. The exponent reads:

$$\lambda_L = \frac{r_0 v}{r_1 r_5} \sqrt{1 + \frac{r_0^2(r_1^2 + r_5^2)}{2r_1^2 r_5^2} \cosh(2\Sigma)}. \quad (5.16)$$

In terms of the Hawking temperature (5.3) and left-/right- moving temperatures $T_{L,R} = \frac{1}{2\pi} \frac{r_0 e^{\pm\Sigma}}{r_1 r_5}$ we can recast this result in the following form (we set $v = 1$)

$$\lambda_L = 2\pi T \cosh \Sigma \sqrt{1 + \pi^2 (r_1^2 + r_5^2) (T_L^2 + T_R^2)}. \quad (5.17)$$

In the dilute gas regime (when $r_0, r_0 \cosh \Sigma \ll r_1, r_5$) the quantity $\pi^2 (r_1^2 + r_5^2) (T_L^2 + T_R^2) = \frac{r_0^2(r_1^2+r_5^2)}{2r_1^2 r_5^2} \cosh(2\Sigma)$ is small, so we can expand the previous equality

$$\lambda_L = 2\pi T \cosh \Sigma \left(1 + \frac{\pi^2}{2} (r_1^2 + r_5^2) (T_L^2 + T_R^2) + \dots \right) \quad (5.18)$$

Importantly, the Lyapunov exponent *does not equal the chaos bound*. It depends on $r_{1,5}$ and $T_{L,R}$ in addition to T , and its temperature dependence is a nonlinear function. But the leading term in the expansion has a simple form:

$$\lambda_L^{(0)} \approx \frac{r_0}{r_1 r_5} = 2\pi T \cosh \Sigma. \quad (5.19)$$

This result is the leading-order term of the dilute-gas expansion, thus in the dilute gas regime the near-horizon Lyapunov exponent is $\lambda_L = 2\pi T \cosh \Sigma$.⁴ This value differs from MSS bound [2] by a factor of $\cosh \Sigma$ which equals unity when $\Sigma = 0$, i.e. when there is no rotation. In absence of rotation the MSS bound is saturated, as expected from our previous analysis of Lyapunov exponent for open string in near-horizon limit of AdS-Schwarzschild black holes.

We can translate our result into the standard variables for rotating BTZ solutions. Since in standard coordinates for BTZ black holes we have $\Omega = w_-/Lw_+$, using Eq. (5.6) it follows that $L\Omega = \tanh \Sigma$. Therefore, after exploiting another trivial identity $\cosh \Sigma = 1/\sqrt{1 - \tanh^2 \Sigma}$, we get

$$\lambda_L = \frac{2\pi T}{\sqrt{1 - L^2 \Omega^2}}, \quad L\Omega \in [0, 1). \quad (5.20)$$

We could express this results in terms of the left and right temperature $T_{L,R}$, making use of the relation $2/T = 1/T_L + 1/T_R \Rightarrow T = 2T_L T_R / (T_L + T_R)$. However, we do not get a particularly simple or more intuitive form than (5.20), which in fact nicely shows how a nonzero rotation rate Ω deforms us away from the universal $2\pi T$ scaling.

⁴One may worry whether this expression remains finite in the near-extremal limit where we take $\Sigma \rightarrow \infty$. We should pay attention to the fact that there is a factor of r_0 hiding inside the temperature T . In the near-extremal limit we also take a limit $r_0 \rightarrow 0$, while keeping $r_0 \cosh \Sigma$ fixed.

This result should be compared to the one found in [71], where chaos in dual CFT was studied by calculating the OTOC correlators of rotating BTZ black holes. The calculation done in [71] obtains two different Lyapunov exponents $\lambda_L^\pm = 2\pi T/(1 \mp L\Omega)$ in the presence of rotation, one of which is above the MSS bound and the other one below it, presuming that $\Omega \neq 0$. Our result (5.20) turns out to be exactly equal to the geometric mean of $\{\lambda_L^+, \lambda_L^-\}$, implying that $\lambda_L^- < \lambda_L < \lambda_L^+$. Both results suggest that in systems without rotational invariance the MSS scale should be modified.

We note in passing that our near-horizon analysis yields a single Lyapunov exponent, rather than a Lyapunov spectrum with two (in general different) exponents as one would expect in this background (and as [71] finds in the rotating BTZ case) – rotation breaks isotropy so the two directions normal to the invariant plane should be inequivalent. This could be because the quanta of p -momentum in D1-D5-p are only left-moving, thus we only see the Lyapunov exponent associated with the temperature of left-moving modes.

5.3.2 Far from horizon

Now we consider the opposite limit when $r \gg r_0, r_0 \cosh \Sigma$ and $r \gg r_1, r_5$. In this case Eq. (5.11) reduces to

$$R^2 \left(v^2 - R'^2 + RR'' \right) = 0. \quad (5.21)$$

There is the trivial solution $R = 0$ and we can write a variational equation around it by putting $R(\sigma) \sim \epsilon + \delta R(\sigma)$, leading to

$$\delta R'' + \frac{2v^2}{\epsilon} \delta R = 0. \quad (5.22)$$

This is a harmonic oscillator (with positive frequency squared) thus the Lyapunov exponent is zero: we have a vanishing Lyapunov exponent in this region. This makes sense, as we already noted that we can think of six-dimensional black string as an interpolation between $\text{AdS}_3 \times \mathbb{S}^3$ and Minkowski spacetime. The far region corresponds to the latter.

So far we have found that the Lyapunov exponent of the unstable (but integrable) saddle point on the horizon depends on the rotation rate and in general differs from the MSS bound when the symmetry of the background is reduced. We have also seen, comparing to [71], that the bulk Lyapunov exponent is not related to the chaos exponent of field-theoretical OTOC. Now we will relate it to the retarded propagator of the string endpoint, i.e. quasiparticle in contact with a thermostat.

5.4 Retarded Green's function in the static limit

Our goal is to find the retarded Green's function dual to the fundamental open static string in the bulk, which is known [33, 34] to correspond to a heavy quasiparticle interacting with a thermal background.⁵ While such a calculation is maybe the most elementary application of AdS/CFT there is, in the D1-D5-p geometry it poses some formal problems. Therefore we go step by step and start from the *static limit* of the *IR propagator*, i.e. we compute the propagator $\tilde{\mathcal{G}}_R(\omega = 0)$ in the near-horizon area, leaving the question of

⁵In the context of D1-D5 CFT it does not make sense to talk of quarks as the symmetries of the theory are different.

matching to the UV regime, i.e. finding the propagator for the UV-complete theory for the next section.⁶

To make the calculations easier, we make the coordinate transformation

$$r \mapsto \frac{r_0^2}{r^2} \equiv \zeta, \quad (5.23)$$

which in our setup also acts as field redefinition.⁷ In the new coordinate ζ , the boundary is located at $\zeta = 0$ while the horizon $r = r_0$ is at $\zeta = 1$. We can rewrite Eq. (5.11) in new coordinates:

$$4v^2 f(Z) h^2(Z) Z^3 (1 - 2 \cosh^2 \Sigma Z) + 4v^2 f'(Z) h^2(Z) Z^4 (-1 + \cosh^2 \Sigma Z) + r_0^2 f^2(Z) \left((2h(Z) + Zh'(Z)) Z'^2 - 2h(Z) Z Z'' \right) = 0, \quad (5.24)$$

$$f(\zeta) = 1 + \frac{r_1^2 + r_5^2}{r_0^2} \frac{1}{\zeta} + \frac{r_1^2 r_5^2}{r_0^4} \frac{1}{\zeta^2}, \quad h(\zeta) = 1 - \zeta. \quad (5.25)$$

This equation can be solved numerically, as shown in Fig. 5.1 where we have plotted two numerical solutions with the same parameters (r_0, r_1, r_5, Σ), but with different boundary conditions at the horizon (Dirichlet vs. Neumann). Both solutions reach the horizon (that was not the case for the open string in AdSS background). Therefore, the correct physical solution is the one with the Neumann condition – it still feels the heat bath but also has vanishing energy density at the horizon, keeping it stable.

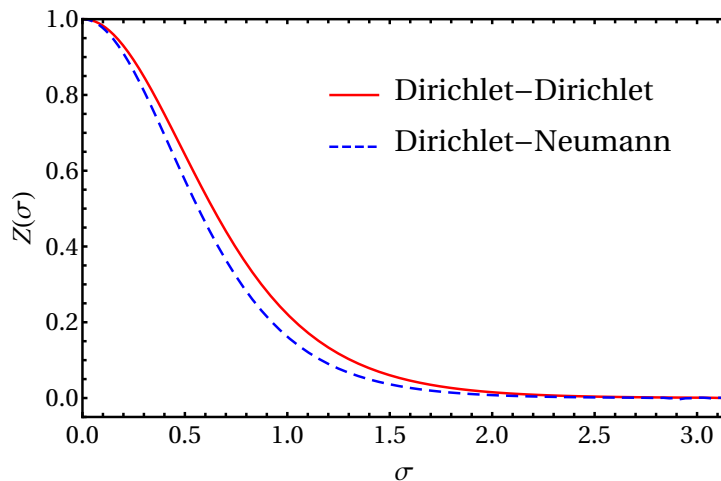


Figure 5.1: Radial profile of the static open string $Z(\sigma)$ in the coordinates from Eq. (5.23), obtained by solving numerically the equation of motion (5.24), with parameters $r_0 = 10$, $r_1 = 100$, $r_5 = 200$, $\Sigma = 1$. On AdS boundary only the Dirichlet boundary condition is meaningful; in the interior both conditions (Dirichlet or Neumann) are possible and both solutions end at the horizon, but the Dirichlet-Neumann solution (blue) has a lower energy than the Dirichlet-Dirichlet solution (red).

We want to find an approximate analytic solution to the equation of motion in the near-horizon region, and then also for the fluctuation equation which determines the Green's

⁶With some hindsight, we denote this propagator by $\tilde{\mathcal{G}}_R$, with a tilde, leaving the notation \mathcal{G}_R for a slightly different correlation function, obtained from transverse fluctuations, to be studied in the next section.

⁷Notice that ζ as defined here differs from the more usual z coordinate in AdS space defined as $z = 1/r$.

function. We will attempt to do so via the matching procedure, namely by solving the relevant equation in two distinct regions (far and near the horizon) and matching them in-between [40, 41]. The matching region is at small σ , since we the boundary at $\sigma = 0$. The matching condition is the nontrivial Virasoro constraint \mathcal{F} which plays the role analogous to the Wronskian for quantum-mechanical scattering problems (i.e., a conserved quantity which stays constant all the way from the near region to the far region):

$$\mathcal{F} \equiv v^2 (-1 + \cosh^2 \Sigma Z) - \frac{(r_1^2 + r_0^2 Z)(r_5^2 + r_0^2 Z) Z'^2}{4r_0^2(Z-1)Z^5} = 0, \quad \frac{d\mathcal{F}}{d\sigma} = 0. \quad (5.26)$$

Substituting $Z \sim 1 + \delta Z(\sigma)$ into Eq. (5.24), we find the fluctuation equation:

$$\delta Z'' - \frac{2r_0^2 v^2 a^4}{(r_0^2 + r_1^2)^2 (r_0^2 + r_5^2)^2} \delta Z = 0. \quad (5.27)$$

A general solution is again a combination of modes with Lyapunov exponents of equal absolute value and opposite signs:

$$\delta Z_{\text{near}} = \mathcal{A} e^{2\lambda_L \sigma} + \mathcal{B} e^{-2\lambda_L \sigma}, \quad \lambda_L = 2\pi T v \cosh \Sigma. \quad (5.28)$$

We also want the solution in the far region. In the far region the leading-order approximation for the on-shell solution is $Z = 0$, so we can expand around it near the boundary $z = 0$:

$$\left[1 + \left(-\frac{3}{2} + 2r_0^2 \left(\frac{1}{r_1^2} + \frac{1}{r_5^2} \right) \right) Z \right] Z'^2 - Z Z'' = 0, \quad (5.29)$$

and put in $Z \sim \epsilon + \delta Z(\sigma)$, yielding simply $-\epsilon \delta Z'' = 0$ with the general solution

$$\delta Z_{\text{far}} = \mathcal{C} \sigma + \mathcal{D}. \quad (5.30)$$

Now we use (5.26) to match the two solutions:

$$Z_{\text{near}} = 1 + \mathcal{A} e^{2\lambda_L \sigma} + \mathcal{B} e^{-2\lambda_L \sigma}, \quad (5.31)$$

$$Z_{\text{far}} = \mathcal{C} \sigma + \mathcal{D}. \quad (5.32)$$

We first evaluate \mathcal{F} for Z_{near} and Z_{far} and then equate them to get

$$\mathcal{C} = 1 + \mathcal{A} e^{2\pi\lambda_L} + \mathcal{B} e^{-2\pi\lambda_L}. \quad (5.33)$$

Expanding the near-region solution in the far region around $\sigma = 0$ yields

$$Z_{\text{near}} = 1 + \mathcal{S} + \mathcal{R} \sigma + \mathcal{O}(\sigma)^2, \quad \mathcal{S} \equiv \mathcal{A} + \mathcal{B}, \quad \mathcal{R} = 2(\mathcal{A} - \mathcal{B}) \lambda_L. \quad (5.34)$$

Now equating the near- and far-region solutions we get

$$\mathcal{A} = -\frac{1 - \mathcal{C}}{2} + \frac{\mathcal{D}}{4\lambda_L}, \quad (5.35)$$

$$\mathcal{B} = -\frac{1 - \mathcal{C}}{2} - \frac{\mathcal{D}}{4\lambda_L}. \quad (5.36)$$

Finally, after combining the results from Eqs. (5.33), (5.35) and (5.36) we get

$$\mathcal{A} = \frac{\mathcal{D}}{2\lambda_L(1 - e^{2\pi\lambda_L})} \quad (5.37)$$

$$\mathcal{B} = \mathcal{A} e^{2\pi\lambda_L}, \quad (5.38)$$

yielding the following form of retarded Green's function at $\omega = 0$

$$\tilde{\mathcal{G}}_R(\omega = 0) = \frac{\mathcal{R}}{\mathcal{S}} = -2\lambda_L \tanh(\lambda_L \pi), \quad \text{Im} \tilde{\mathcal{G}}_R(\omega = 0) = 0. \quad (5.39)$$

This is by construction the time-independent solution, as we have ignored the τ -dependence from the very beginning. We notice that the IR Green's function at $\omega = 0$ is *purely real* – there is no imaginary part, implying there is no absorption at $\omega = 0$. We will understand the meaning of this surprising fact in the next section. Before that, let us make it clear what quantity we study by computing \mathcal{G}_R – on the gravity side, the imaginary part of the propagator is the absorption cross section for an open string (i.e., the probability that the horizon absorbs a probe string) – this is distinct from the familiar greybody factor computed in [65] which is the absorption cross section for the Hawking radiation; its CFT meaning is the transparency of the thermal plasma to radiation. The greybody factor is certainly nonzero; why the dissipation for a heavy quark is zero we shall understand when we do the calculation also for $\omega \neq 0$.

5.5 Dynamics of transverse fluctuations

Now we want to obtain the retarded Green's function for a general ω value. It is quite challenging to solve for time-dependent fluctuations δR in the Polyakov gauge. Instead, we will consider a slightly different setup (and thus a different Green's function): we switch to the Nambu-Goto formalism with the action (3.2) and work in the static gauge, so that instead of studying perturbations in the radial direction of the string, we will now consider a setup in which only the fluctuations along the x_5 -direction are present. That will allow us to study t -dependent dynamics. A similar calculation was already done in a slightly different setup [72], where the authors study the bulk dynamics of a fundamental string in an extremal and near-extremal Reissner-Nordström black hole background.

The ansatz is now:

$$\begin{aligned} t(\tau, \sigma) &= \tau \equiv t, & R(\tau, \sigma) &= \sigma \equiv r, \\ \Psi(\tau, \sigma) &\equiv \psi(t), & \Theta(\tau, \sigma) &\equiv \pi/2, & \Phi(\tau, \sigma) &\equiv \phi(t), & X_5(\tau, \sigma) &\equiv X(t, r). \end{aligned} \quad (5.40)$$

We expand $X(t, r)$ in Fourier modes

$$X(t, r) = \int \frac{d\omega}{2\pi} e^{-i\omega t} X_\omega(r), \quad (5.41)$$

and the relevant equation of motion obtained by varying the Nambu-Goto action reads

$$\begin{aligned} X_\omega''(r) + \left(\frac{r_0^2 (-3r^2 + r_0^2 + (r^2 - r_0^2) \cosh^2(2\Sigma))}{r(r^2 - r_0^2)(-2r^2 + r_0^2 + r_0^2 \cosh^2(2\Sigma))} - \frac{f'(r)}{f(r)} + \frac{h'(r)}{2h(r)} \right) X_\omega'(r) \\ - \frac{2r^2 \omega^2 f(r)}{(-2r^2 + r_0^2 + r_0^2 \cosh^2(2\Sigma)) h(r)} X_\omega(r) = 0. \end{aligned} \quad (5.42)$$

In the special case when there is no rotation ($\Sigma = 0$) this equation simplifies to

$$X_\omega''(r) + \left(\frac{r_0^2}{r^3 h(r)} - \frac{f'(r)}{f(r)} + \frac{h'(r)}{2h(r)} \right) X_\omega'(r) + \frac{\omega^2 f(r)}{h^2(r)} X_\omega(r) = 0. \quad (5.43)$$

From now on we will assume that there is no rotation. Since the problem can be divided into two regions, we will again employ the matching procedure in order to gain some analytic control of the equation.

5.5.1 Near region: extremal case

We first consider the near-horizon region of the extremal black string, i.e. at temperature $T = 0$ on the field theory side. In this case the IR geometry is given by Eqs. (5.4). The relevant equation of motion for string fluctuations along the x_5 -direction in this regime is

$$X_\omega''(r) + \frac{4}{r}X_\omega'(r) + \left(\frac{L^2\omega}{r^2}\right)^2 X_\omega(r) = 0, \quad (5.44)$$

with general solutions of the form

$$X_\omega(r) = \mathcal{A} \left(1 - \frac{iL^2\omega}{r}\right) e^{\frac{iL^2\omega}{r}} + \mathcal{B} \frac{1}{2L^4\omega^2 r} \left(1 - \frac{ir}{L^2\omega}\right) e^{-\frac{iL^2\omega}{r}}. \quad (5.45)$$

Imposing the infalling boundary condition (appropriate for the retarded propagator) at the horizon requires $\mathcal{B} = 0$. Expanding this solution in the matching region $r_0 \ll r \ll L$, we get

$$X_\omega(r) = \mathcal{A} \left(1 + \frac{(L^2\omega)^2}{r^2}\right). \quad (5.46)$$

From this we can calculate retarded Green's function at $T = 0$ in the IR region $r_0/r, \omega L \ll 1 \ll L/r$:

$$\mathcal{G}_R^{(T=0)} = L^4\omega^2 \Rightarrow \text{Im } \mathcal{G}_R^{(T=0)} = 0. \quad (5.47)$$

Therefore, we again get a vanishing absorption cross-section in the presence of the horizon, i.e. $\text{Im } \mathcal{G}_R^{(T=0)} = 0$. While for $\omega = 0$ this could be ascribed to the special static limit, now we need to understand why the extremal horizon does not absorb anything even though it is a horizon (with finite area and finite greybody factor). From the bulk viewpoint, one way to see the reason is to rewrite the fluctuation equation (5.44) in the Schrödinger form:

$$\partial_r^2 \tilde{X}_\omega(r) - V_{\text{eff}}(r) \tilde{X}_\omega(r) = 0, \quad V_{\text{eff}}(r) = \frac{2r^2 - L^4\omega^2}{r^4}. \quad (5.48)$$

The effective potential is shown in Fig. 5.2 for various values of ω . For $\omega = 0$ a zero imaginary part could be expected for two reasons. First, for $\omega = 0$ the effective potential is positive and (quadratically) divergent at the horizon, thus there is no absorption, i.e. all incoming waves are reflected backward. Also, we have already studied the $\omega = 0$ case (though for radial fluctuations) and shown that $\text{Im } \tilde{\mathcal{G}}_R = 0$ at all temperatures.

The nonstatic case $\omega \neq 0$ is more interesting. As we see from Eq. (5.48) and Fig. 5.2, the potential is now attractive (negative) and diverges as $1/r^4$ for $r \rightarrow 0$. It is known that the scattering problem for attractive central potentials diverging as $1/r^s$ for $s > 2$ is not well-defined [73]: such potentials always lead to a wave "falling toward the center" and the solution to the Schrödinger equation in this case is always localized around zero – there is no absorption because the infalling plane wave at infinity is not a consistent boundary condition. We will see in the following section that we can infer the result for the retarded Green's function in the extremal case by considering the limit $\omega \ll T$ of the thermal correlator obtained in a near-extremal case.

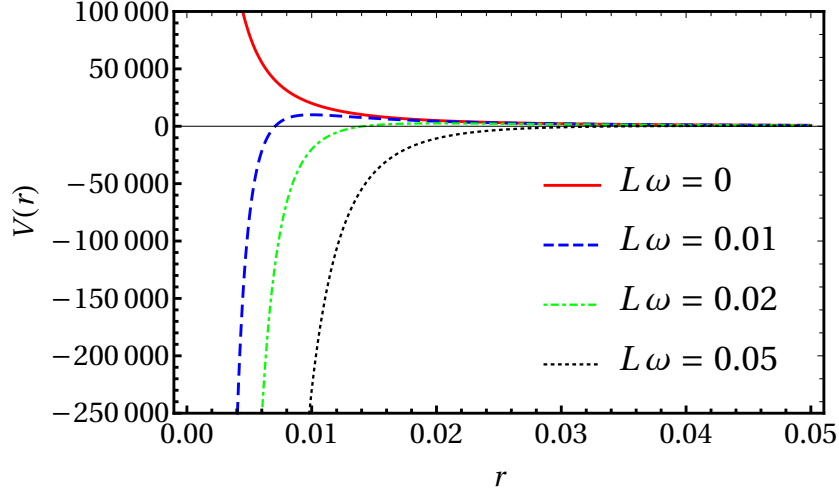


Figure 5.2: The effective Schrödinger potential (5.48) for the extremal D1-D5 geometry with $L = 1$, for four values of the frequency ω . The static case $\omega = 0$ (red full line) is qualitatively different because the potential is strongly repulsive: there is no absorption because plan waves coming from infinity are reflected away. For $\omega > 0$ (blue, green, black dotted lines) the potential is strongly attractive, diverging as $1/r^4$ at the origin $r = 0$. This again implies zero absorption cross section as there are no solutions behaving as plane waves at infinity.

5.5.2 Near region: near-extremal case

At low but finite temperatures or equivalently in the near-extremal case we would be interested in dynamics of open string in the metric given by Eq. (5.5). Therefore, we look for the solution of open string equations in $\text{BTZ} \times \mathbb{S}^3$ geometry. For simplicity we assume that there is no rotation ($\Sigma = 0$). The relevant equation can be written in a compact form reminiscent to the relativistic wave equation in curved background:

$$\frac{h(r)}{r^4} \frac{d}{dr} \left(h(r) r^4 \frac{dX_\omega(r)}{dr} \right) + \frac{L^4 \omega^2}{r^4} X_\omega(r) = 0. \quad (5.49)$$

It is again instructive to look at the Schrödinger form of the equation, obtained by plugging in $X_\omega(r) = h^{-1/2}(r) r^{-2} \Psi(r)$ into Eq. (5.49):

$$\left(\frac{d^2}{dr^2} - V_{\text{eff}}(r) \right) \Psi(r) = 0, \quad V_{\text{eff}}(r) = \frac{2r^2 - 3r_0^2 - L^4 \omega^2}{(r^2 - r_0^2)^2}. \quad (5.50)$$

The second term inside the brackets is the effective Schrödinger potential, plotted in Fig. 5.3.

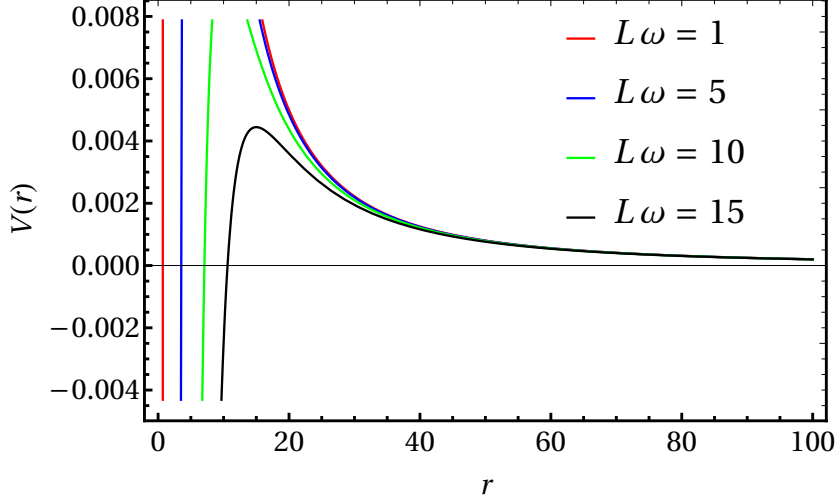


Figure 5.3: The effective Schrödinger potential (5.50) for a near-extremal D1-D5-p system with the parameters $r_0 = 0.1$, $L = 1$, for $L\omega = 1, 5, 10, 15$ (red, blue, green, black). Already from the expression in Eq. (5.50) it is obvious that in the near-extremal case nothing special happens in the static limit $\omega = 0$. For all frequencies, the potential has the form typical of near-horizon effective potentials [40, 41], where a high but finite potential barrier is followed by the infinite well at the horizon $r = r_0$.

Proceeding further toward the analytic solution to Eq. (5.49) we again change the radial variable to $\zeta = r_0^2/r^2$, as in Eq. (5.23). In order to reduce Eq. (5.49) to a hypergeometric differential equation,⁸ we will make a further coordinate transformation $\zeta \mapsto 1 - \xi$. The equation now reads

$$X_\omega''(\xi) - \frac{1}{2\xi} \frac{2-\xi}{1-\xi} X_\omega'(\xi) + \frac{1}{\xi^2(1-\xi)} \left(\frac{L^2\omega}{2r_0} \right)^2 X_\omega(\xi) = 0. \quad (5.51)$$

We can solve this equation at the horizon $\xi = 0$, by making the substitution $y = -\log \xi$ in Eq. (5.51). The solution at the horizon takes the form $X_\omega \sim e^{\pm i\alpha y} = \xi^{\pm i\alpha}$, with $\alpha = L^2\omega/2r_0$. The boundary condition at the horizon requires the outgoing modes to vanish, yielding

$$X_\omega(\xi) = \tilde{\mathcal{A}} \xi^{-i\alpha}. \quad (5.52)$$

In order to get the full near-horizon solution, we plug the ansatz $X_\omega(\xi) = \xi^{-i\alpha} F(\xi)$ into Eq. (5.51), yielding

$$\xi(1-\xi) \frac{d^2 F}{d\xi^2} + \left[1 - 2i\alpha - \left(1 - i\alpha - \frac{1}{2} - i\alpha \right) \xi \right] \frac{dF}{d\xi} - (-i\alpha) \left(-\frac{1}{2} - i\alpha \right) F(\xi) = 0, \quad (5.53)$$

where the parameter $\alpha = L^2\omega/2r_0$ is the same that we encountered in the solution at the horizon. We recognize Eq. (5.53) as the hypergeometric equation with parameters

$$a = -i\alpha, \quad b = -\frac{1}{2} - i\alpha, \quad c = 1 - 2i\alpha. \quad (5.54)$$

The corresponding regular solution reads

$$F(\xi) = \tilde{\mathcal{A}} {}_2F_1(a, b, c; \xi) + \tilde{\mathcal{B}} \xi^{2i\alpha} {}_2F_1(a+1-c, b+1-c, 2-c; \xi). \quad (5.55)$$

⁸Since Eq. (5.49) has three regular singular points at $r = 0$, r_0 and ∞ , we can be sure that it can be written in the form of the hypergeometric differential equation.

We impose the infalling boundary condition (5.52) at the horizon, implying that $\tilde{\mathcal{B}} = 0$, thus the near-horizon solution becomes

$$X_\omega(\xi) = \tilde{\mathcal{A}} \xi^{-i\alpha} {}_2F_1(a, b, c; \xi). \quad (5.56)$$

This completes the near-region solution.

We can now use the following identity to express solution (5.56) in terms of functions depending on ζ , instead of $\xi = 1 - \zeta$:

$$\begin{aligned} {}_2F_1(a, b, c; \xi) &= \frac{\Gamma(c)\Gamma(c-a-b)}{\Gamma(c-a)\Gamma(c-b)} {}_2F_1(a, b, 1+a+b-c; \zeta) + \\ &+ \frac{\Gamma(c)\Gamma(a+b-c)}{\Gamma(a)\Gamma(b)} \zeta^{c-a-b} {}_2F_1(c-a, c-b, 1+c-a-b; \zeta). \end{aligned} \quad (5.57)$$

The matching region $r_0 \ll r$ corresponds to $\zeta \ll 1$, so we expand Eq. (5.57) in small ζ :

$${}_2F_1(a, b, c; \xi) \approx \frac{\Gamma(c)\Gamma(c-a-b)}{\Gamma(c-a)\Gamma(c-b)} + \frac{\Gamma(c)\Gamma(a+b-c)}{\Gamma(a)\Gamma(b)} \zeta^{c-a-b}, \quad (5.58)$$

We observe that the full solution in the matching region is of the form

$$X_\omega(r) \propto \tilde{\mathcal{S}} r^{-d+\Delta} + \tilde{\mathcal{F}} r^{-\Delta}, \quad d = \Delta = 3, \quad (5.59)$$

which allows us to read off the retarded Green's function as the ratio $\tilde{\mathcal{F}}/\tilde{\mathcal{S}}$:

$$\mathcal{G}_R^{(T)}(\omega) \propto \frac{\Gamma(c-a)\Gamma(c-b)}{\Gamma(a)\Gamma(b)} = \frac{\Gamma\left(1 - i\frac{\omega}{2\lambda_L}\right) \Gamma\left(\frac{3}{2} - i\frac{\omega}{2\lambda_L}\right)}{\Gamma\left(-i\frac{\omega}{2\lambda_L}\right) \Gamma\left(-\frac{1}{2} - i\frac{\omega}{2\lambda_L}\right)}. \quad (5.60)$$

We can take the imaginary part of (5.60) to get the absorption cross-section:

$$\sigma_{\text{abs}} = \text{Im} \mathcal{G}_R^{(T)}(\omega) \propto \frac{\alpha}{4} + \alpha^3, \quad \alpha = \frac{\omega}{2\lambda_L}, \quad \lambda_L = 2\pi T. \quad (5.61)$$

This is the central result of our calculation – the IR propagator and the absorption cross section for a heavy quasiparticle. Let us think what this result means:

1. The only energy scale in the Green's function is the MSS scale $2\pi T$. This is despite the fact that the system has two independent scales (r_1/r_0 and r_5/r_0 or equivalently T and Ω) and despite the fact that the greybody factor depends nontrivially on all three whereas the bulk Lyapunov exponent depends on two of them.
2. This is in line with the problem of drift of a heavy quark through neutral $\mathcal{N} = 4$ super-Yang-Mills (SYM) plasma, dual to a dragging string in AdSS background [33, 34, 74] and many subsequent works in the same setup [75, 76, 77, 78, 79]: the D1-D5 quasiparticle also does not see the charges of the D1-D5-p system, it does not even see the global rotation.⁹ This can be ascribed to the fact that the additional charges of D1-D5-p system are global and the quasiparticle is neutral with respect to them.

⁹At least, this is the case in our current setup with no drift; it would be interesting to check if this conclusion remains in force in presence of drift.

3. The form of the propagator (Eq. 5.60) could be expected from the BTZ asymptotics of the near-extremal geometry [80], as it has the form of conformal quantum mechanics, i.e. 0+1-dimensional CFT [81] (we know that in the near-horizon region of the BTZ geometry the transverse spatial coordinate decouples and the geometry becomes $\text{AdS}_2 \times \mathbb{S}$, so that AdS_2 gives the 0+1-dimensional CFT).
4. The imaginary part behaving as $\sim \omega + \omega^3$ suggests that in addition to the usual drag force $f \propto \dot{x}$ we have also a third-order term $f \propto dx^3/dt^3$. This is in fact expected – all odd-power terms¹⁰ in velocity are allowed symmetry-wise and the leading-order holographic Green function already captures the first two terms.
5. This result could not be reproduced either from the static limit nor from the extremal limit – these two limits are singular, which is expected for the static limit but somewhat strange for the extremal limit.

As a sanity check we consider the high-frequency limit $\omega \gg T$ where one should get a result for the extremal case.¹¹ In this limit we can compare our calculation to the pure CFT result for the two-point correlation function. We consider a two-point correlation function in a 2+1-dimensional CFT for an operator with scaling dimension Δ : this behaves as $\langle \mathcal{O}_\Delta(t) \mathcal{O}_\Delta(0) \rangle \sim |t|^{-2\Delta}$, i.e. $\sim \omega^{2\Delta-d}$, where d is the spacetime dimensionality. For an operator with a scaling dimension $\Delta = 3$ living in $d = 3$ spacetime dimensions, one should indeed expect $\sim \omega^3$ power-law behavior of the thermal correlator in the high-frequency limit.

5.5.3 Signals of instability

What else can we learn from the two-point thermal correlator (5.60) that would be relevant for the main objective of this paper? We should note that poles in the retarded Green's function are related to transport properties of the thermal field theory; on the gravity side, they define a spectrum of quasinormal modes (QNM) [40, 41]. More specifically, the relaxation times in field theory are given by the imaginary part of the QNM spectrum in the bulk [82, 83]. Since our retarded Green's function (5.60) is singular at an infinite number of points in the complex plane, due to the presence of the gamma functions in the numerator, we can extract the whole QNM spectrum from it. Singular points are given by $c - a = -n$ or $c - b = -n$, for $n \in \mathbb{Z}^+$ (a set of non-negative integers), thus $\omega_n = -2i(n+1)\lambda_L$ or $\omega_n = -2i(n+3/2)\lambda_L$. Considering the union of the two sets yields the following spectrum:

$$\omega_n = -2i(\mathbf{n} + 1)\lambda_L, \quad \mathbf{n} = 0, \frac{1}{2}, 1, \frac{3}{2}, \dots \quad (5.62)$$

or equivalently

$$\omega_m = -i(\mathbf{m} + 1)\lambda_L, \quad \mathbf{m} = 1, 2, 3, \dots \quad (5.63)$$

¹⁰Even-power terms (like \dot{x}^2) are not expected as their sign is independent of the sign of velocity, i.e. a proper drag force (opposing the motion) would have to look like $-\dot{x}^2 \text{sgn} \dot{x}$ but that implies the breaking of some discrete symmetry which we do not have.

¹¹In this limit we consider wavelengths well below T^{-1} ($\omega^{-1} \ll T^{-1}$) that are insensitive to thermal fluctuations and thus resemble the behavior for extremal background geometry.

We write the solution in these two obviously equivalent ways in order to facilitate the comparison with the literature.¹² Another way to derive the QNM spectrum is directly from the solutions to the equations of motion by imposing the infalling boundary condition at the horizon and the Dirichlet boundary condition at the boundary. The latter requires the solution at infinity to vanish.¹³ The equivalence of the two approaches should be obvious, since the same set of requirements that force the solution (5.58) to vanish at infinity also describe the poles of the retarded Green's function (5.60). This gives us a more intuitive picture of QNM: they tell us how a local near-horizon instability decays. Therefore, we can think of the inverse of the Lyapunov exponent λ_L^{-1} as some characteristic timescale for decay of perturbations along the open string that has nothing to do with chaos.

This result is qualitatively the same as the one obtained by for scalar perturbations in a nonrotating BTZ black hole background [82], except that the spectrum (5.63) also includes half-integer values of n . More importantly, a similar relationship between QNM and the Lyapunov exponent was found in the studies of null unstable geodesics in quite general *asymptotically flat* backgrounds (more precisely, for any stable, stationary, spherically symmetric and asymptotically flat spacetime) [59]. The message of [59] is that the instability timescale of the geodesic motion is related to the inverse of the Lyapunov exponent, thus we can think of our work as stringy generalization of their result in asymptotically AdS spaces.

Finally, we should also comment on the field theory interpretation of quasi-normal modes spectrum that we have just found in the bulk. We already mentioned that an open string in the bulk stretched from the boundary to the thermal horizon via gauge/gravity duality corresponds to a heavy quasiparticle in thermal plasma. Perturbations along the string describe thermal perturbations in the plasma. We can summarize the findings from above by noting that a Lyapunov exponent is really related to the quasi-normal modes frequencies, which describe how local near-horizon instabilities on the string decay. Decay rates of those instabilities are given by the spectrum of quasi-normal modes, so on the field theory side they describe how thermal fluctuations in plasma die off. Thus, they predict thermalization timescale of a quasiparticle as a thermal perturbation of a thermal state describing the background plasma at a finite temperature in the dual CFT theory [82].

5.5.4 Far region solution

Now that we have the IR propagator the usual recipe would be to obtain also the propagator in the UV regime and perform the matching procedure between the near- and far-region solution. We will now explain why this fails for the D1-D5-p system. We first need a quantity conserved along the radial direction which provides the matching condition. This is typically the Wronskian of the two independent bulk solutions. The Wronskian for Eq. (5.43) is

$$\mathcal{W}[\psi_1, \psi_2; r] = \frac{h(r)}{f(r)} [\psi_1 \partial_r \psi_2 - \psi_2 \partial_r \psi_1], \quad \partial_r \mathcal{W} = 0. \quad (5.64)$$

¹²The form (5.63) is simpler and more natural but (5.62) has the same form as the scalar QNM solution [82] that we want to benchmark against.

¹³On the other hand, in an asymptotically Minkowski spacetime we would require outgoing boundary condition at infinity.

We shall see soon that the far-region solution corresponds to the usual near-boundary behavior of a scalar in AdS but with a plane-wave modulation along the radial direction. Far from horizon ($r \gg r_0$), Eq. (5.42) reduces to

$$X_\omega''(r) + \frac{2(r^2(r_1^2 + r_5^2) + 2r_1^2 r_5^2) X_\omega'(r)}{r(r^2 + r_1^2)(r^2 + r_5^2)} + \frac{(r^2 + r_1^2)(r^2 + r_5^2) \omega^2 X_\omega(r)}{r^4} = 0. \quad (5.65)$$

In order to implement the low-energy condition $\omega r_1, \omega r_5 \ll 1$, we make the substitutions $X_\omega(r) \equiv r^{-3/2} \psi(r)$ and $\rho = \omega r$, yielding

$$\begin{aligned} & -(\rho^2 + \omega^2 r_1^2)(\rho^2 + \omega^2 r_5^2) \psi(\rho) + \frac{\rho^2 \omega^2 ((r_1^2 + r_5^2) \rho^2 + 2r_1^2 r_5^2 \omega^2) (3\psi(\rho) - 2\rho\psi'(\rho))}{(\rho^2 + \omega^2 r_1^2)(\rho^2 + \omega^2 r_5^2)} - \\ & - \frac{15}{4} \rho^2 \psi(\rho) - \rho^3 (-3\psi'(\rho) + \rho\psi''(\rho)) = 0, \end{aligned} \quad (5.66)$$

from which the low-energy conditions $\omega r_{1,5} \ll 1$ together with the obvious inequality $\omega r_{1,5} \frac{r_{1,5}}{r} \ll 1$ imply

$$\left(1 + \frac{15}{4\rho^2}\right) \psi(\rho) - \frac{3}{\rho} \psi'(\rho) + \psi''(\rho) = 0, \quad (5.67)$$

with a general solution

$$\psi(\rho) = \rho^{3/2} (C_1 e^{-i\rho} + C_2 e^{i\rho}). \quad (5.68)$$

This implies that $X_\omega = r^{3/2} \psi \sim r^0 \times (\exp(i\rho) + \exp(-i\rho))$. The leading r^0 behavior is just what we expect from the IR region and the identification of the string worldsheet field as a massless scalar, however the rapidly oscillating terms for $r \rightarrow \infty$ cannot be matched to the IR expansion. This can happen – there is guarantee that the convergence radii of the IR and UV expansion overlap. In this case the full propagator can only be found numerically, however we postpone that for further work. The key information of interest (the thermalization timescale and the role of the MSS bound) can be seen already from the IR calculation.

On the other hand, in holography we always want to decouple the IR region from the the UV region, since it corresponds to the Minkowski spacetime. One typically invokes a so called Maldacena's decoupling limit in order to decouple from the asymptotically flat region. In that case we are not interested in dynamics of the UV region, so we should not worry much about the failure to perform the full matching procedure. We can think of the matching region $r \gg r_0$ as the limit in which we reach the boundary of AdS spacetime, where holographic recipe for calculating correlation functions is well defined. Therefore, what we call the IR propagator is really a full holographic 2-point function.

Chapter 6

Spectrum of rotating strings and energy-angular momentum relations

6.1 Introduction

We explore the meaning of dynamical instability and chaos for spinning closed strings in $\text{AdS}_5 \times \mathbb{S}^5$ geometry. Such strings have a transparent meaning in dual field theory: a string corresponds to a composite operator with large conformal dimension Δ in dual CFT, usually interpreted as glueballs and other bound states in QCD terminology [32, 84, 85, 86, 87, 88, 89, 90, 91, 92, 93, 94, 95, 96, 97, 98] (of course, we know that the dual of $\text{AdS}_5 \times \mathbb{S}^5$ is really the SYM theory, but the QCD analogy remains useful at least for gaining intuition). The rotation rate in AdS and on the sphere \mathbb{S} correspond to the spin S and orbital momentum J of a field theory state, thus the rotating closed string defines the energy E of a bound state with spin S and angular momentum J .

In general, one might worry that even at large 't Hooft coupling the gauge operators with high conformal dimension might be beyond the scope of classical strings on supergravity backgrounds. However, at large angular momenta S and J the conformal dimension Δ is likewise large but such operators are amenable to classical description in string theory on the classical $\text{AdS}_5 \times \mathbb{S}^5$ background. As it was shown in [84], the corresponding string states are solitonic solutions, describing precisely the rotating closed string configurations.¹ Computing the spectrum yields a relation $E = E(J, S)$, bearing in mind that $E \sim \Delta$ at large Δ . In planar space (instead of $\text{AdS}_5 \times \mathbb{S}^5$), this yields the celebrated relation $E^2 \sim S$ (at $J = 0$), describing the Regge trajectory of massive hadrons. In AdS (and on the sphere), one explores different corners of the parameter space; some predictions, like the logarithmic corrections to deep inelastic scattering, can be checked directly in gauge theory [84, 89, 92, 99] while others are novel and go beyond what is possible in field theory [32, 86, 93, 95].

Here we show that one can go further in exploring the spectra of high-spin gauge operators (or generalized Regge trajectories) from the *classical* string dynamics viewpoint. This case is very different from the open string dynamics considered in the rest of the paper: closed rotating strings exhibit nonintegrable dynamics and chaos in the presence of horizon, they do not generically reach neither the deep interior (or horizon, at finite temperature) nor the boundary, and thus do not relate to the MSS bound which is a

¹They are solitonic in the sense that they are classical but not perturbatively related to the static string, i.e. the trivial vacuum

characteristic of thermal horizons.

The plan is as follows. We first introduce the setup (geometry, string action and ansatz) for a spinning closed string in $\text{AdS}_5 \times \mathbb{S}^5$, then we derive the variational equations and compute their growing (Lyapunov) modes, and finally show what they mean in CFT: they describe the thermodynamic response to the relevant operators which grow in the IR and deform the CFT, modifying in turn the Regge relations $E = E(J, S)$.

6.2 Setup

6.2.1 Closed spinning string

We consider the global $\text{AdS}_5 \times \mathbb{S}^5$ geometry, i.e. the whole geometry dual to the $\mathcal{N} = 4$ SYM field theory:

$$\begin{aligned} ds_{\text{AdS}_5}^2 &= -\cosh^2 \rho dt^2 + d\rho^2 + \sinh^2 \rho d\Omega_3^2 \\ d\Omega_3^2 &= d\theta_1^2 + \cos^2 \theta_1 (d\theta_2^2 + \cos^2 \theta_2 d\theta_3^2) \\ ds_{\mathbb{S}^5}^2 &= d\phi_1^2 + \cos^2 \phi_1 (d\phi_2^2 + \cos^2 \phi_2 d\tilde{\Omega}_3^2) \\ d\tilde{\Omega}_3^2 &= d\phi_3^2 + \cos^2 \phi_3 (d\phi_4^2 + \cos^2 \phi_4 d\phi_5^2). \end{aligned} \quad (6.1)$$

Here, the coordinate ρ parametrizes the radial direction in global AdS, varying from $\rho = 0$ (interior) to $\rho = \pi/2$ (boundary), t is the usual time coordinate, θ_i ($i = 1, \dots, 3$) parametrizes the 3-sphere slice of constant time and radial distance in AdS, and ϕ_i ($i = 1, \dots, 5$) parametrizes the 5-sphere. The Polyakov action reads:

$$S_P = -\frac{1}{2\pi\alpha'} \int d\tau d\sigma \eta^{\alpha\beta} \partial_\alpha X^\mu \partial_\beta X^\nu G_{\mu\nu}(X). \quad (6.2)$$

In order to account both for the $SO(4)$ gauge symmetry and the $SO(6)$ R-symmetry of the SYM dual, we need to have a string spinning both in AdS, with spin S (encoding for the gauge charge) and on the five-sphere, with spin J (encoding for the R-charge). This setup, studied in [85] corresponds to the following closed string ansatz in the (τ, σ) worldsheet coordinates [85]:

$$\begin{aligned} t &= v\tau, \quad \rho = \rho(\sigma), \quad \Theta_3 = \omega\tau, \quad \Phi_5 = \nu\tau \\ \Theta_1 &= \Theta_2 = \Phi_1 = \Phi_2 = \Phi_3 = \Phi_4 = 0. \end{aligned} \quad (6.3)$$

The sole nontrivial equation of motion and the nontrivial constraint read

$$\rho'' + \frac{\omega^2 - v^2}{2} \sinh 2\rho = 0 \quad (6.4)$$

$$\rho'^2 - v^2 \cosh^2 \rho + \omega^2 \sinh^2 \rho + \nu^2 = 0. \quad (6.5)$$

In constructing the solution we closely follow the well-known works [84, 85, 86, 32, 90]. The string rotates along one angle in AdS and one angle on the 5-sphere while keeping a rigid shape (radial profile). Explicit solution to Eqs. (6.4-6.4) can be found in terms of Jacobi elliptic functions as we already did for a slightly different closed string ansatz (ring string) in [23]:

$$\rho(\sigma) = \arccos \text{cn} \left(\sqrt{\omega^2 - \nu^2} \sigma, \frac{\omega^2 - v^2}{\omega^2 - \nu^2} \right). \quad (6.6)$$

This solution has the form of an elongated closed curve with one end at $\rho = 0$ and the other end at $\rho = \rho_0$ which can be computed from Eq. (6.5) by putting $\rho'(\pi/2) = 0$ (or directly from the solution (6.6) by putting $\sigma = \pi/2$):

$$\rho_0 = \operatorname{arth} \frac{v^2 - \nu^2}{\omega^2 - \nu^2}. \quad (6.7)$$

Thus ρ_0 is the farthest UV scale the string reaches. Short strings, having $\nu \lesssim v$, only explore a small part of AdS space and to a first approximation see the deep interior of AdS as almost flat. Long strings, with $\nu \lesssim \omega$, on the contrary explore almost the whole AdS space and thus contain almost the full spectrum of the gauge theory. Intermediate cases fit interpolate between these two extremes.

The energy and angular momenta are given by the conserved worldsheet currents corresponding to translations along t , θ_3 and ϕ_5 (we first give the general expression and then evaluate it for the ansatz (6.3)):

$$E = \frac{1}{2\pi\alpha'} \int d\sigma \int d\sigma t \cosh^2 \rho = \frac{v}{\pi\alpha'} \int d\sigma \cosh^2 \rho(\sigma) \quad (6.8)$$

$$S = \frac{1}{2\pi\alpha'} \int d\sigma \cos^2 \Theta_1 \cos^2 \Theta_2 \dot{\Theta}_3 \sinh^2 \rho = \frac{\omega}{\pi\alpha'} \int d\sigma \sinh^2 \rho(\sigma) \quad (6.9)$$

$$J = \frac{1}{2\pi\alpha'} \int d\sigma \cos^2 \Phi_1 \cos^2 \Phi_2 \cos^2 \Phi_3 \cos^2 \Phi_4 \dot{\Phi}_5 = \frac{\nu}{\pi\alpha'} \quad (6.10)$$

The pathway found in [89] to explicitly write down the values of the integrals is to write $d\sigma = d\rho/\rho'$ and express ρ' from the constraint. This yields

$$E = \frac{v}{\pi\alpha'} \int d\rho \frac{\cosh^2 \rho}{\sqrt{-\nu^2 + v^2 \cosh^2 \rho - \omega^2 \sinh^2 \rho}} \quad (6.11)$$

$$S = \frac{\omega}{\pi\alpha'} \int d\rho \frac{\sinh^2 \rho}{\sqrt{-\nu^2 + v^2 \cosh^2 \rho - \omega^2 \sinh^2 \rho}} \quad (6.12)$$

$$J = \frac{\nu}{\pi\alpha'} \int d\rho \frac{1}{\sqrt{-\nu^2 + v^2 \cosh^2 \rho - \omega^2 \sinh^2 \rho}}. \quad (6.13)$$

These complicated expressions still tell us little. The strategy in [84] and many subsequent works is to consider separately the case of short and long strings, and for each of these the limit of large vs. small orbital momentum J , i.e. angular velocity ν . The following regimes are identified:

1. For short strings ($\nu \lesssim v$) and small ν , we have $E^2 - J^2 \sim (2/\alpha')S$ – the regime of the canonical Regge slope as the short string does not see the curvature of the AdS space.
2. For short strings ($\nu \lesssim v$) and large ν , we have $E - J - S \sim (1/2\alpha')S/J^2$.
3. For long strings ($\nu \lesssim \omega$) and small ν , we have $E - S \sim (1/\pi\alpha') \log(S/\alpha') + (\pi/2\alpha')J^2/\log(S/\alpha')$, the log-correction characteristic of theories with gauge invariance.
4. For long strings ($\nu \lesssim \omega$) and large ν , we have $E - S - J \sim 1/(\pi^2\alpha'^2) \log(S/J)/J$, again a logarithmic correction, as long strings see that curvature of AdS which encodes for the gauge invariance.

One needs to resort to numerical integration in order to interpolate between these extremal cases. We are however mainly interested in the long string regime, where both the classical gravity limit of the bulk description and the planar limit of the CFT description are well-defined. To remind, our goal now is not so much to arrive at new predictions for the gauge theory but to understand the gauge theory meaning of the bulk instability.

6.2.2 Closed winding spinning string

The alternative configuration that we study is that of a winding spinning string, considered e.g. in [89, 92, 95]. In this case, in addition to the rotation of Θ_3 and Φ_5 , we also allows Θ_1 to wind n times. This string has interesting dynamics and in the non-rotational case it can violate the MSS bound for $n > 1$ [23]. Here we will encounter this solution as a stable fixed point toward which the systems evolves starting from a non-winding spinning string in some parameter regime. The winding ansatz reads

$$\begin{aligned} t = v\tau, \quad \rho = \rho(\sigma), \quad \Theta_1 = \Theta_1(\sigma), \quad \Theta_2 = \omega_2\tau, \quad \Theta_3 = \omega_3\tau, \quad \Phi_5 = v\tau \\ \Phi_1 = \Phi_2 = \Phi_3 = \Phi_4 = 0. \end{aligned} \quad (6.14)$$

The equations of motion and the constraint read:

$$\rho'' - \frac{1}{2} \sinh^2 \rho (v^2 - \omega_2^2 \sin^2 \Theta_2 - \omega_3^2 \sin^2 \Theta_3) = 0 \quad (6.15)$$

$$\Theta_1'' + 2\rho' \coth \rho \Theta_1' + \frac{\omega_2^2 - \omega_3^2}{2} \sin 2\Theta_1 = 0 \quad (6.16)$$

$$\rho^2 + \sinh^2 \rho (\Theta_1')^2 - v^2 \cosh^2 \rho + (\omega_2^2 \sin^2 \Theta_1 + \omega_3^2 \cos^2 \Theta_2) \sinh^2 \rho = 0. \quad (6.17)$$

We now follow [89] which finds that $\omega_2 = \omega_3 \equiv \omega$ is a necessary condition to make the system analytically solvable. In this case, writing out the equations of motion, one finds that $\rho = \rho_0 = \text{const.}$ so that the string stays at fixed distance from the horizon. The solution is now easily found to be

$$\rho(\sigma) = \text{arsh} \frac{v}{n\sqrt{2}}, \quad \Theta_1(\sigma) = n\sigma, \quad \omega = \sqrt{v^2 + n^2}. \quad (6.18)$$

The conserved currents can now be found directly from Eqs. (6.8-6.10), without the need for the trick from Eqs. (6.11-6.13). We focus now on the small J case, which again can be studied in the short- and long-string regime:

1. For a short string ($v \ll 1$) we have the flat-space Regge trajectory with a subleading correction: $E^2 - J^2 - 2\sqrt{S} = 2S^{(3/2)} + \dots$, as a short string barely feels the curvature.
2. For a long string ($v \gg 1$) we have the relation $E - 2S - 2J = 2^{3/2}S^{1/3}$.

In this system there are no log-corrections, as the gauge operator is more complicated: it is not a single-trace but a double-trace operator and its gauge transformation properties are different [96]. Now we will study the stability of both systems and find how the saddle-point instability of the string describes the RG flow.

6.3 Lyapunov exponents and the deformations of the gauge theory

6.3.1 Variational equations and their solutions

Closed spinning string

The strategy is the same as before: we find the variational equations by definition and then we compute finite-time/finite-distance Lyapunov exponents. It is not hard to see that the variational equations of the worldsheet fields Φ_1 to Φ_4 are all equal, and likewise those for Θ_1 and Θ_2 . We thus consider the variational system for $\delta\Theta_2$, $\delta\Phi_4$ and $\delta\rho$; we find that turning on $\delta\Theta_3$ and $\delta\Phi_5$ does not lead to interesting consequences (it merely renormalizes ω and ν). We take the ansatz

$$\delta\rho = \delta\rho(\sigma), \quad \delta\Theta_2 = \delta\Theta_2(\tau, \sigma), \quad \delta\Phi_4 = \delta\Phi_4(\tau, \sigma), \quad (6.19)$$

which is the most general form of the variations which still allows the separation of variables. It turns out that the only possible form of $\delta\Theta_2$ is $\delta\Theta_2 = \exp(-i\omega t)\delta\theta_2(\sigma)$ for some Ω . The variational equations read

$$\delta\rho'' + (\omega^2 \cosh 2\rho - v^2 \cosh 2\rho) \delta\rho = 0 \quad (6.20)$$

$$\delta\theta_2'' + 2 \coth \rho \rho' \delta\theta_2' + (\Omega^2 - \omega^2) \delta\theta_2 = 0 \quad (6.21)$$

$$\delta\ddot{\Phi}_4 - \delta\Phi_4'' + \nu^2 \delta\Phi_4 = 0. \quad (6.22)$$

We seek the solutions that start from given (small) variation ϵ in the IR and grow. Absorbing ϵ into the amplitude of the variations for simplicity, the solutions read:²

$$\delta\rho(\sigma) = \frac{1 - \frac{\sigma}{\pi/2}}{\cosh(\sqrt{\omega^2 - v^2}\sigma)} - \frac{2}{\pi\sqrt{\omega^2 - v^2}} \sinh(\sqrt{\omega^2 - v^2}\sigma) \quad (6.23)$$

$$\delta\theta_2(\sigma) = \cosh(\sqrt{\omega^2 - v^2}\sigma) {}_2F_1\left(\frac{1}{2}, \frac{1}{2} + \frac{1}{\sqrt{\omega^2 - v^2}}, \frac{3}{2}, \cosh^2(\sqrt{\omega^2 - v^2}\sigma)\right) \quad (6.24)$$

$$\delta\Phi_4(\tau, \sigma) = \exp^{-i\omega\tau} \sin(\nu\sigma). \quad (6.25)$$

As we see, the variation of the orbital momentum ($\delta\Phi_4$) is harmonic in both τ and σ and the corresponding Lyapunov exponent is zero. The radial and the spin Lyapunov exponents read $\lambda_\rho = \sqrt{\omega^2 - v^2}$ and $\lambda_{\Theta_2} = 2 + 6\sqrt{\omega^2 - v^2}$, which is easily obtained by expanding the solutions. However, the exponents by themselves mean little in this setup, also because there is no horizon and thus no universal scale.

Closed spinning winding string

For the winding string we try the same ansatz (6.19) for the variations as for the non-winding case. The equations of motion read

$$n^2 \sqrt{2 + \frac{v^2}{n^2}} \delta\rho' + \frac{v}{2} \sqrt{n^2 + v^2} \sin(2n\sigma) \delta\dot{\Theta}_2 = 0 \quad (6.26)$$

$$2n \cos(n\sigma) \delta\Theta_2' + \sin(n\sigma) (\delta\Theta_2'' - \delta\ddot{\Theta}_2) = 0 \quad (6.27)$$

$$\delta\ddot{\Phi}_4 - \delta\Phi_4'' + \nu^2 \delta\Phi_4 = 0. \quad (6.28)$$

²We will restore the ϵ dependence later when analyzing how the dispersion relations change due to the growing instability.

The second equation implies that the only way the variables can be separated is to have $\delta\Theta_2 = \delta\Theta_2(\sigma)$ and $\delta\rho = \delta\rho_0 = \text{const.}$ when the variation of the AdS angle is found to be

$$\delta\Theta_1(\sigma) = \frac{e^{-i\Omega\sigma}}{\sin(n\sigma)}. \quad (6.29)$$

For the 5-sphere angle Φ_4 , the variational equation is the same as before, thus the solution is also the same as in Eq. (6.25). The Lyapunov exponents of the spinning winding string are obviously $\lambda_\rho = \lambda_\Theta = \lambda_\Phi = 0$ – there is no exponentially growing mode.

6.3.2 Deformations of the spectrum of the gauge operators

The response of the energy spectrum is obtained by replacing $(\rho, \Theta_1, \Theta_2, \Phi_4) \mapsto (\rho + \delta\rho, \Theta_1 + \delta\Theta_1, \Theta_2 + \delta\Theta_2, \Phi_4 + \delta\Phi_4)$ in the expressions (6.8-6.10), plugging in the solutions (6.23-6.25) for the non-winding case, or (6.29) for the winding case, linearizing in the fluctuations and integrating. We will now show that the growing modes ($\delta\rho$ and $\delta\Theta_2$) describe the deformation of the spinning solution at constant radius $\rho = \rho(\sigma)$ toward the new solution with lower energy (essentially, the tunnelling from false to true vacuum).

Short string regime. In the short string regime, the Regge-like behavior is stable and the variations merely renormalize E and S . We can see this by a double expansion of $E + \delta E$ and $S + \delta S$ in ϵ and $1/\nu$. The resulting expression yields the off-shell dispersion relation:

$$E^2 - J^2 = \frac{2}{\alpha'} S + \epsilon e^{-i\frac{\omega}{\nu}t} \left(E^2 - J^2 - \frac{2}{\alpha'} S \right) = 0. \quad (6.30)$$

In other words, the dispersion relation remains the same upon renormalizing

$$(E, S, J) \rightarrow (E(1 + \epsilon e^{-i\frac{\omega}{\nu}t}), S(1 + \epsilon e^{-i\frac{\omega}{\nu}t}), J(1 + \epsilon e^{-i\frac{\omega}{\nu}t})). \quad (6.31)$$

Averaging over time, the renormalization actually averages to zero but even at any fixed time instant, the dispersion relation does not change (since we multiply all the currents by $1 + \epsilon$). The Regge bound state is thus a line of fixed points (the perturbation neither grows nor decays). This is indeed known from gauge theory which is shown in [92] by computing the full quadratic perturbation Lagrangian and diagonalizing the system of fluctuation equations. Here we show it in a much simpler way, solving three decoupled equations and without any formal stability analysis.

Long strings regime. In this regime the spin perturbation grows with the Lyapunov exponents λ_ρ and λ_{Θ_2} which behave as $\sim \sqrt{\omega^2 - v^2} \gg 1$. We thus expect that an instability will develop. Inserting the variations into the expressions for (E, S, J) , one finds

$$(E-S) \left(1 + \epsilon e^{-i\frac{\omega}{\nu}t + 2\sqrt{\omega^2 - v^2}t} \right) - J = \frac{1}{2\pi\alpha'} \left[S \left(1 + \epsilon e^{-i\frac{\omega}{\nu}t + 2\sqrt{\omega^2 - v^2}t} \right) \right]^{1/3} \left(1 + \epsilon e^{-i\frac{\omega}{\nu}t + 2\sqrt{\omega^2 - v^2}t} \right)^{2/3} + \dots \quad (6.32)$$

meaning that, for large ω , the terms proportional to the exponential dominate even for ϵ small, yielding

$$E - S = \frac{1}{2\pi\alpha'} S^{1/3} + \dots, \quad (6.33)$$

exactly the same dispersion relation as for the winding string. While the instability of the long-string regime is again known from the literature [85, 90] where it was computed in the SYM theory, it is not known what the correct vacuum is – our result, based on

studying the leading growing modes, suggests it is in fact the multi-trace operator dual to the winding string. Notice that J is irrelevant and only gives subdominant contributions in the new vacuum, i.e. the stable point is the single-spinning string. It would be interesting to study how far one can go in understanding this in gauge theory.

We can now repeat the stability analysis for the the winding string itself. We will be brief as the algorithm is exactly the same. For the *short-string* regime, despite zero Lyapunov exponents, the system has an instability related to the fact that the perturbation $\delta\Theta_1$ as given in Eq. (6.29) becomes large for small σ although it is not exponentially large but only linearly. The dispersion relation is dominated by this small- σ contribution and reads

$$E - 2S - 2J = \frac{\alpha'}{n} S^2 + \dots, \quad (6.34)$$

which at leading order reproduces the long-string regime but the correction is different and depends on the winding. We do not know what this regime means in CFT. For the *long string*, the story is the same as for the short string without winding (Eq. 6.31), i.e. the original dispersion relation stays the same, multiplied by a renormalization factor. This fixed point is thus stable. Therefore, a long non-winding double-spinning string will evolve toward a long winding single-spinning string and stay there. This can also be directly checked numerically.

6.4 Discussion and conclusions

What have we done? We have solved for linearized perturbations around the spinning string solutions. Linearized fluctuation equations that we solve are just a special case (with special boundary conditions) of the general quadratic fluctuation Lagrangian around the classical solution, considered e.g. in [85, 94]. The general quadratic fluctuation Lagrangian (i.e., general linearized fluctuation equations) are the framework for the leading quantum correction to the classical soliton solution, exploited in [85] and many subsequent works to obtain the leading finite 't Hooft coupling corrections in the gauge theory spectrum.

However, we study the equations with different boundary conditions, looking solely at the leading growing mode. This correctly predicts the instability of the state created by a spin-2 single-trace operator, which evolves toward a state created by a spin-1 multi-trace operator (since the theory is conformal at zero temperature, we are allowed to make such identifications of states with operators). Therefore, the Lyapunov stability analysis for closed strings is really the RG analysis in gauge theory. This is different from the straight open string, where it characterizes the thermalization timescale – but in fact, in the latter case we can also say that the quark evolves from a pure (non-thermal) state toward a mixed state corresponding to the thermal regime, and the Lyapunov exponent measures how rapidly this happens.

Chapter 7

Discussion and conclusions

The initial motivation for this work was a rather technical question: what is the meaning of bulk chaos in particle and string motion in AdS spaces, and why it typically saturates the same universal chaos bound as OTOC in field theory. We were led to the study of open strings (rather than ring strings or particle geodesics) largely by reasons of calculational simplicity and direct CFT interpretation: a string with one end on the boundary and the other in the interior describes the motion of a heavy quark in quark-gluon plasma. The holographic interpretation is less obvious for other string configurations, and for geodesics it corresponds to a rather special, high-conformal-dimension limit.

As usual, the chase is almost better than the catch. We have found a number of surprising properties of bulk dynamics – integrability of open string motion as opposed to closed strings, horizon as an unstable saddle point and the "fake nest of chaos" with local instability rate exactly equal to the MSS bound $2\pi T$ in the static case but different from it in the rotating black string geometry. But the holographic interpretation is equally interesting: the universal MSS scale is a red herring, the artifact of the large- N limit in field theory, i.e. classical bulk dynamics, when temperature is the only scale, unless some additional symmetry is explicitly broken. This happens in the D1-D5-p black string, where the rotation breaks the symmetry between left- and right-moving modes. Just like in [100], the rotating system deforms away from the MSS exponent, and this shows directly in the correlation functions. We also note that away from the dilute gas approximation there are additional higher-order in temperature corrections to the Lyapunov exponent that will violate MSS bound.

An interesting connection, or maybe we should better call it a generalization, to the particle motion in a simple asymptotically flat static black hole background is found. A non-vanishing Lyapunov exponent can be assigned to null unstable geodesics and was found to be related to the spectrum of quasi-normal modes [59]. In that scenario, a Lyapunov exponent describes an instability scale of null unstable geodesics. Our calculation of a thermal correlator for transverse fluctuations of an open string in the non-rotational limit of black string background also reveals a similar relationship between the poles of a correlator, namely a spectrum of quasi-normal modes, and the Lyapunov exponent saturating the universal MSS bound. This gives us an important hint to answer our question about the meaning of the bulk Lyapunov exponent: it is an instability scale associated to the decay of fluctuations along the string due to thermal dissipation, and has nothing to do with bulk chaos.

At the end of the day, the variation and its growth rate (i.e., the bulk Lyapunov exponent) is nothing but the linearized fluctuation about the on-shell solution, the bread and

better of holographic calculations, that defines correlation functions like susceptibilities, conductivities and similar. The difference between these calculations and the equation for the bulk Lyapunov exponent is that the initial condition is different. The Lyapunov variation has a prescribed small value at $t = 0/\sigma = 0$, and is given by the growing branch for long times/worldsheet distances, unlike the usual correlation functions which are determined by other boundary conditions:

1. In time, the boundary conditions in the IR determine the contour choice for the correlation function.
2. In the radial coordinate, they are dictated by stability requirements, i.e. the finiteness of the stress-energy tensor.

The Lyapunov growing mode in time violates (i) – the contour choice – so it determines some other correlation functions rather than the textbook ones (retarded, advanced, etc), but we have seen in Chapter 5 that the MSS scale will show up in all two-point correlators, e.g. in G_R . The Lyapunov growing mode in the radial coordinate violates (ii) – the stability requirement – so its meaning is precisely that of an RG flow from an unstable to a stable fixed point, as we show in Chapter 6.

Finally, the issue of gauge choice might be worth commenting. Our choice to work in the conformal gauge instead of static gauge most of the time is somewhat unusual. The static gauge equates the time and radial coordinate with the worldsheet coordinates τ and σ and thus immediately kills the unphysical (gauge-dependent) degrees of freedom. But the conformal gauge has several advantages for us: (i) it simplifies many calculations (ii) it allows us to look at the fluctuations along the holographic RG flow (the radial direction) which, as we have seen, have an interesting interpretation in field theory (iii) it does not fully fix the reparametrization invariance on the worldsheet, leaving the $SL(2, \mathbb{R})$ group of global coordinate transformations, but as argued in [42, 43, 49] this group provides a nice way to understand the appearance of the universal MSS scale and its disappearance when we determine the boundary conditions for the transverse fluctuations that fully fix the gauge on the worldsheet. This approach was exploited in full depth in [49] to study quantum chaos, i.e. OTOC on the worldsheet of the open string.

Appendix A

Trivial dynamics of time-dependent fluctuations

Here we show that the static open string/heavy quark does not exhibit any instability in the time-dependent fluctuations of the transverse coordinates. In other words, the sole nontrivial dynamics is that of radial fluctuations, studied in the main text. We work in the static gauge but now allowing arbitrary dynamics along the x_1 -direction (for simplicity we ignore the remaining transverse coordinates as they decouple at linear order):

$$t = \tau, \quad R = \sigma, \quad X_1 = X_1(\tau, \sigma), \quad X_i = 0, \quad i = 2, \dots, D - 1. \quad (\text{A.1})$$

The only nontrivial equation of motion for this ansatz is for X_1 , obtained from the Nambu-Goto action (3.2) as

$$-2\sigma^4 h'(\sigma) X_1' - 2\sigma^3 h(\sigma) (4X_1' + \sigma X_1'') + \frac{2\ddot{X}_1}{h(\sigma)} = 0. \quad (\text{A.2})$$

If we assume a straight string $X_1 = X_1(\tau)$, the above equation becomes completely trivial, reducing to $X_1'' = 0$. A generalization with harmonic radial dependence $X_1 = \tilde{X}_1(\tau) \exp(ik\sigma)$ turns out to be inconsistent with Eq. (A.2). If we assume instead a static but non-straight string $X_1 = X_1(\sigma)$, that brings us back to the ansatz from the main text (in different gauge). Leaving the fully general dependence on both t and r yields solutions which can exhibit spatiotemporal chaos and possibly turbulence [101]; while very interesting on its own, this situation is beyond the scope of this paper.

Appendix B

Symmetries of AdS₃ and BTZ spaces

We can describe AdS₃ spacetime as a hyperboloid surface embedded in four-dimensional flat spacetime with a metric signature $(-, +, +, -)$ [102]

$$G_{AB}X^AX^B \equiv -X_0^2 + X_1^2 + X_2^2 - X_3^2 = -L^2, \quad (\text{B.1})$$

where L is the curvature radius of this surface. In global coordinates (t, ρ, ϕ) we can define the following mapping

$$X_0 = L \cosh \rho \cos t, \quad X_1 = L \sinh \rho \sin \phi, \quad X_2 = L \sinh \rho \cos \phi, \quad X_3 = L \cosh \rho \sin t, \quad (\text{B.2})$$

that gives us the induced metric describing AdS₃ in global coordinates

$$ds^2 \equiv g_{\mu\nu}dx^\mu dx^\nu = -L^2 (\cosh^2 \rho dt^2 + d\rho^2 + \sinh^2 \rho d\phi^2). \quad (\text{B.3})$$

Besides the derivation of the metric coefficients, describing AdS space as an embedded hyperboloid in flat space can be used to extract Killing vectors by projecting vector fields from flat space onto the lower-dimensional surface. The projection operator

$$\mathcal{P}^\mu{}_A = g^{\mu\nu}G_{AB} \frac{\partial X^B}{\partial x^\nu}. \quad (\text{B.4})$$

takes the A -component of a vector field living in flat space and projects it to the μ -component of the vector field living on the embedded surface. Since we are interested in symmetries, we will consider the Killing vector fields on the previously described flat spacetime. They form a Lie algebra $\mathfrak{so}(2, 2)$ with four boost generators

$$\chi_i = X_0\partial_i + X_i\partial_0, \quad \bar{\chi}_i = X_3\partial_i + X_i\partial_3, \quad i = 1, 2, \quad (\text{B.5})$$

and two generators of rotation

$$\xi = X_1\partial_2 - X_2\partial_1, \quad \bar{\xi} = X_0\partial_3 - X_3\partial_0. \quad (\text{B.6})$$

Altogether we have six symmetry generators as one should expect, since AdS spacetime is maximally symmetric with the maximal number of symmetry generators $(d(d+1)/2)$ in d spacetime dimensions. We now act on these vector fields (B.5-B.6) with the projection operator (B.4):

$$V_1 = \mathcal{P}^\mu{}_A \chi_1^A \partial_\mu = -\sin t \sin \phi \tanh \rho \partial_t + \cos t \sin \phi \partial_\rho + \cos t \cos \phi \coth \rho \partial_\phi \quad (\text{B.7})$$

$$V_2 = \mathcal{P}^\mu{}_A \chi_2^A \partial_\mu = -\sin t \cos \phi \tanh \rho \partial_t + \cos t \cos \phi \partial_\rho - \cos t \sin \phi \coth \rho \partial_\phi \quad (\text{B.8})$$

$$V_3 = \mathcal{P}^\mu{}_A \bar{\chi}_1^A \partial_\mu = \cos t \sin \phi \tanh \rho \partial_t + \sin t \sin \phi \partial_\rho + \sin t \cos \phi \coth \rho \partial_\phi \quad (\text{B.9})$$

$$V_4 = \mathcal{P}^\mu{}_A \bar{\chi}_2^A \partial_\mu = \cos t \cos \phi \tanh \rho \partial_t + \sin t \cos \phi \partial_\rho - \sin t \sin \phi \coth \rho \partial_\phi \quad (\text{B.10})$$

$$V_5 = \mathcal{P}^\mu{}_A \xi^A \partial_\mu = -\partial_\phi \quad (\text{B.11})$$

$$V_6 = \mathcal{P}^\mu{}_A \bar{\xi}^A \partial_\mu = \partial_t. \quad (\text{B.12})$$

In order to show that the isometries of AdS_3 form the $\mathfrak{so}(2, 2) \cong \mathfrak{sl}_2 \times \mathfrak{sl}_2$ algebra we define two sets of vector fields:

$$\zeta_{\pm} = \frac{1}{2} (V_1 + V_4 \mp i (V_2 - V_3)), \quad \zeta_0 = \frac{1}{2} (-V_5 + V_6), \quad (\text{B.13})$$

$$\bar{\zeta}_{\pm} = \frac{1}{2} (V_1 - V_4 \mp i (V_2 + V_3)), \quad \bar{\zeta}_0 = \frac{1}{2} (V_5 + V_6). \quad (\text{B.14})$$

For readers' convenience we write down the resulting components of the Killing vectors ζ_{\pm} and ζ_0 :¹

$$\zeta_{\pm} = \frac{1}{2} (e^{\pm i(t+\phi)} \tanh \rho \partial_t \mp e^{\pm i(t+\phi)} \partial_{\rho} + e^{\pm i(t+\phi)} \coth \rho \partial_{\phi}), \quad (\text{B.15})$$

$$\zeta_0 = \frac{1}{2} (\partial_t + \partial_{\phi}). \quad (\text{B.16})$$

One can easily check that under the action of the Lie bracket $\{, \}_{\text{L.B.}}$ these generators will satisfy the \mathfrak{sl}_2 Lie algebra

$$i\{\zeta_+, \zeta_-\}_{\text{L.B.}} = 2\zeta_0, \quad i\{\zeta_{\pm}, \zeta_0\}_{\text{L.B.}} = \pm\zeta_{\pm}. \quad (\text{B.17})$$

This is the symmetry algebra for AdS_3 spaces. We are also interested in near- AdS_3 spaces, namely BTZ black hole spacetimes. Since (non-rotating) BTZ is locally AdS_3 it will also possess the same symmetry generators. We have learned from [42, 43] that under certain circumstances, the maximal chaos exponent is a consequence of \mathfrak{sl}_2 near-horizon symmetry algebra, as was mentioned in the main text.

¹The other set of Killing vectors, namely the bared ones, would be the same up to $\phi \rightarrow -\phi$.

Appendix C

Conserved charges in AdS₃ gravity

Quasilocal stress-energy tensor can be defined at the boundary of AdS space [68]. In the case of three-dimensional AdS it reads

$$8\pi T_{\mu\nu} = K_{\mu\nu} - \left(K + \frac{1}{L}\right) \gamma_{\mu\nu}, \quad (\text{C.1})$$

where $\gamma_{\mu\nu}$ is the induced metric on the boundary, $K_{\mu\nu}$ is its extrinsic curvature tensor and K is its trace. We can use this stress tensor to calculate conserved charges. Given a Killing vector ζ^μ that leaves the boundary metric unchanged, the corresponding conserved charge is

$$Q_\zeta = \int_{\partial\text{AdS}_3} d^2x \sqrt{\gamma} (u^\mu T_{\mu\nu} \zeta^\nu), \quad (\text{C.2})$$

where $\gamma = \det \gamma_{\mu\nu}$ and u^μ is a timelike unit normal to the boundary ∂AdS_3 . Using this method we want to calculate conserved charges of rotating BTZ black hole spacetime (5.7). We expand this solution at the boundary

$$ds_{\text{BTZ}}^2 \approx \frac{w^2}{L^2} (-dt^2 + dx^2) + \frac{L^2 dw^2}{w^2} + \delta g_{\mu\nu} dx^\mu dx^\nu, \quad (\text{C.3})$$

where we keep only the leading terms in $\delta g_{\mu\nu}$:

$$\delta g_{tt} = \frac{w_+^2 + w_-^2}{L^2}, \quad \delta g_{tx} = \frac{w_+ w_-}{L^2}, \quad \delta g_{ww} = \frac{L^2 (w_+^2 + w_-^2)}{w^4}. \quad (\text{C.4})$$

We now compute extrinsic curvature tensor and its trace

$$K_{tt} = -K_{xx} = \frac{w^2}{L^3} - \frac{w_+^2 + w_-^2}{2L^3} + 3 \frac{(w_+^2 + w_-^2)^2}{8L^3 w^2} + \mathcal{O}\left(\frac{1}{w}\right)^3, \quad (\text{C.5})$$

$$K = -\frac{2}{L} + \mathcal{O}\left(\frac{1}{w}\right)^3. \quad (\text{C.6})$$

Therefore, the stress tensor (C.1) becomes

$$T_{tt} = T_{xx} = \frac{w_+^2 + w_-^2}{16\pi L^3} + \mathcal{O}\left(\frac{1}{w}\right)^2, \quad T_{tx} = \frac{w_+ w_-}{8\pi L^3} + \mathcal{O}\left(\frac{1}{w}\right)^2. \quad (\text{C.7})$$

Finally, the conserved charges, namely the energy and angular momentum are

$$E = L \int_0^{2\pi} dx T_{tt} = \frac{w_+^2 + w_-^2}{8L^2} + \mathcal{O}\left(\frac{1}{w}\right)^2, \quad (\text{C.8})$$

$$J = L \int_0^{2\pi} dx T_{tx} = \frac{w_+ w_-}{4L^2} + \mathcal{O}\left(\frac{1}{w}\right)^2. \quad (\text{C.9})$$

Bibliography

- [1] Y. Sekino and L. Susskind, *Fast Scramblers*, *JHEP* **10** (2008) 065, [[arXiv:0808.2096](#)].
- [2] J. Maldacena, S. H. Shenker, and D. Stanford, *A bound on chaos*, *JHEP* **08** (2016) 106, [[arXiv:1503.01409](#)].
- [3] S. H. Shenker and D. Stanford, *Black holes and the butterfly effect*, *JHEP* **03** (2014) 067, [[arXiv:1306.0622](#)].
- [4] D. A. Roberts, D. Stanford, and L. Susskind, *Localized shocks*, *JHEP* **03** (2015) 051, [[arXiv:1409.8180](#)].
- [5] S. H. Shenker and D. Stanford, *Stringy effects in scrambling*, *JHEP* **05** (2015) 132, [[arXiv:1412.6087](#)].
- [6] J. Maldacena and D. Stanford, *Remarks on the Sachdev-Ye-Kitaev model*, *Phys. Rev. D* **94** (2016), no. 10 106002, [[arXiv:1604.07818](#)].
- [7] E. Marcus and S. Vandoren, *A new class of SYK-like models with maximal chaos*, *JHEP* **01** (2019) 166, [[arXiv:1808.01190](#)].
- [8] A. M. García-García, B. Loureiro, A. Romero-Bermúdez, and M. Tezuka, *Chaotic-Integrable Transition in the Sachdev-Ye-Kitaev Model*, *Phys. Rev. Lett.* **120** (2018), no. 24 241603, [[arXiv:1707.02197](#)].
- [9] N. Lashkari, D. Stanford, M. Hastings, T. Osborne, and P. Hayden, *Towards the Fast Scrambling Conjecture*, *JHEP* **04** (2013) 022, [[arXiv:1111.6580](#)].
- [10] A. Almheiri, T. Hartman, J. Maldacena, E. Shaghoulian, and A. Tajdini, *The entropy of Hawking radiation*, *Rev. Mod. Phys.* **93** (2021), no. 3 035002, [[arXiv:2006.06872](#)].
- [11] G. Penington, S. H. Shenker, D. Stanford, and Z. Yang, *Replica wormholes and the black hole interior*, *JHEP* **03** (2022) 205, [[arXiv:1911.11977](#)].
- [12] A. Almheiri, T. Hartman, J. Maldacena, E. Shaghoulian, and A. Tajdini, *Replica Wormholes and the Entropy of Hawking Radiation*, *JHEP* **05** (2020) 013, [[arXiv:1911.12333](#)].
- [13] D. Stanford, *More quantum noise from wormholes*, [arXiv:2008.08570](#).
- [14] P. Saad, S. H. Shenker, D. Stanford, and S. Yao, *Wormholes without averaging*, [arXiv:2103.16754](#).

- [15] P. Saad, S. Shenker, and S. Yao, *Comments on wormholes and factorization*, [arXiv:2107.13130](#).
- [16] J. Pollack, M. Rozali, J. Sully, and D. Wakeham, *Eigenstate Thermalization and Disorder Averaging in Gravity*, *Phys. Rev. Lett.* **125** (2020), no. 2 021601, [[arXiv:2002.02971](#)].
- [17] B. Mukhametzhanov, *Factorization and complex couplings in SYK and in Matrix Models*, [arXiv:2110.06221](#).
- [18] F. S. Nogueira, S. Banerjee, M. Dorband, R. Meyer, J. v. d. Brink, and J. Erdmenger, *Geometric phases distinguish entangled states in wormhole quantum mechanics*, *Phys. Rev. D* **105** (2022), no. 8 L081903, [[arXiv:2109.06190](#)].
- [19] M. Čubrović, *Replicas, averaging and factorization in the IIB matrix model*, *JHEP* **09** (2022) 136, [[arXiv:2203.10697](#)].
- [20] A. Blommaert, L. V. Iliesiu, and J. Kruthoff, *Gravity factorized*, [arXiv:2111.07863](#).
- [21] K. Hashimoto and N. Tanahashi, *Universality in Chaos of Particle Motion near Black Hole Horizon*, *Phys. Rev. D* **95** (2017), no. 2 024007, [[arXiv:1610.06070](#)].
- [22] S. Dalui and B. R. Majhi, *Near horizon local instability and quantum thermality*, *Phys. Rev. D* **102** (2020), no. 12 124047, [[arXiv:2007.14312](#)].
- [23] M. Čubrović, *The bound on chaos for closed strings in Anti-de Sitter black hole backgrounds*, *JHEP* **12** (2019) 150, [[arXiv:1904.06295](#)].
- [24] D.-Z. Ma, D. Zhang, G. Fu, and J.-P. Wu, *Chaotic dynamics of string around charged black brane with hyperscaling violation*, *JHEP* **01** (2020) 103, [[arXiv:1911.09913](#)].
- [25] C. Yu, D. Chen, B. Mu, and Y. He, *Violating the chaos bound in five-dimensional, charged, rotating Einstein-Maxwell-Chern-Simons black holes*, *Nucl. Phys. B* **987** (2023) 116093.
- [26] D. Giataganas, *Chaotic Motion near Black Hole and Cosmological Horizons*, *Fortsch. Phys.* **70** (2022), no. 1 2200001, [[arXiv:2112.02081](#)].
- [27] T. Dray and G. 't Hooft, *The Gravitational Shock Wave of a Massless Particle*, *Nucl. Phys. B* **253** (1985) 173–188.
- [28] T. Dray and G. 't Hooft, *The Effect of Spherical Shells of Matter on the Schwarzschild Black Hole*, *Commun. Math. Phys.* **99** (1985) 613–625.
- [29] P. Kraus, F. Larsen, and S. P. Trivedi, *The Coulomb branch of gauge theory from rotating branes*, *JHEP* **03** (1999) 003, [[hep-th/9811120](#)].
- [30] V. Balasubramanian and S. F. Ross, *Holographic particle detection*, *Phys. Rev. D* **61** (2000) 044007, [[hep-th/9906226](#)].

- [31] J. Louko, D. Marolf, and S. F. Ross, *On geodesic propagators and black hole holography*, *Phys. Rev. D* **62** (2000) 044041, [[hep-th/0002111](#)].
- [32] J. G. Russo, *Anomalous dimensions in gauge theories from rotating strings in $AdS(5) \times S^{**5}$* , *JHEP* **06** (2002) 038, [[hep-th/0205244](#)].
- [33] C. P. Herzog, A. Karch, P. Kovtun, C. Kozcaz, and L. G. Yaffe, *Energy loss of a heavy quark moving through $N=4$ supersymmetric Yang-Mills plasma*, *JHEP* **07** (2006) 013, [[hep-th/0605158](#)].
- [34] S. S. Gubser, *Drag force in AdS/CFT* , *Phys. Rev. D* **74** (2006) 126005, [[hep-th/0605182](#)].
- [35] J. M. Maldacena, *Wilson loops in large N field theories*, *Phys. Rev. Lett.* **80** (1998) 4859–4862, [[hep-th/9803002](#)].
- [36] S.-J. Rey, S. Theisen, and J.-T. Yee, *Wilson-Polyakov loop at finite temperature in large N gauge theory and anti-de Sitter supergravity*, *Nucl. Phys. B* **527** (1998) 171–186, [[hep-th/9803135](#)].
- [37] A. Brandhuber, N. Itzhaki, J. Sonnenschein, and S. Yankielowicz, *Wilson loops in the large N limit at finite temperature*, *Phys. Lett. B* **434** (1998) 36–40, [[hep-th/9803137](#)].
- [38] S.-J. Rey and J.-T. Yee, *Macroscopic strings as heavy quarks in large N gauge theory and anti-de Sitter supergravity*, *Eur. Phys. J. C* **22** (2001) 379–394, [[hep-th/9803001](#)].
- [39] K. Hashimoto, K. Murata, and N. Tanahashi, *Chaos of Wilson Loop from String Motion near Black Hole Horizon*, *Phys. Rev. D* **98** (2018), no. 8 086007, [[arXiv:1803.06756](#)].
- [40] O. Aharony, S. Gubser, J. Maldacena, H. Ooguri, and Y. Oz, *Large N Field Theories, String Theory and Gravity*, *Phys.Rept.* **323** (2000) 183–386, [[hep-th/9905111](#)].
- [41] E. Kiritsis, *String theory in a nutshell*. Princeton University Press, USA, 2019.
- [42] H. W. Lin, J. Maldacena, and Y. Zhao, *Symmetries Near the Horizon*, *JHEP* **08** (2019) 049, [[arXiv:1904.12820](#)].
- [43] H. Lin and D. Stanford, *A symmetry algebra in double-scaled SYK*, [[arXiv:2307.15725](#)].
- [44] S. Dalui, B. R. Majhi, and P. Mishra, *Presence of horizon makes particle motion chaotic*, *Phys. Lett. B* **788** (2019) 486–493, [[arXiv:1803.06527](#)].
- [45] U. H. Danielsson, E. Keski-Vakkuri, and M. Kruczenski, *Vacua, propagators, and holographic probes in AdS / CFT* , *JHEP* **01** (1999) 002, [[hep-th/9812007](#)].
- [46] D. Rodriguez-Gomez and J. G. Russo, *Thermal correlation functions in CFT and factorization*, *JHEP* **11** (2021) 049, [[arXiv:2105.13909](#)].

- [47] D. Rodriguez-Gomez and J. G. Russo, *Correlation functions in finite temperature CFT and black hole singularities*, *JHEP* **06** (2021) 048, [[arXiv:2102.11891](#)].
- [48] J. de Boer, E. Lladrés, J. F. Pedraza, and D. Vegh, *Chaotic strings in AdS/CFT*, *Phys. Rev. Lett.* **120** (2018), no. 20 201604, [[arXiv:1709.01052](#)].
- [49] S. Giombi, S. Komatsu, and B. Offertaler, *Chaos and the reparametrization mode on the AdS₂ string*, [arXiv:2212.14842](#).
- [50] F. Herček, V. Gecin, and M. Čubrović, *Photoemission "experiments" on holographic lattices*, *SciPost Phys. Core* **6** (2023) 027, [[arXiv:2208.05920](#)].
- [51] A. Stepanchuk and A. A. Tseytlin, *On (non)integrability of classical strings in p-brane backgrounds*, *J. Phys. A* **46** (2013) 125401, [[arXiv:1211.3727](#)].
- [52] L. A. Pando Zayas and C. A. Terrero-Escalante, *Chaos in the Gauge / Gravity Correspondence*, *JHEP* **09** (2010) 094, [[arXiv:1007.0277](#)].
- [53] V. E. Korepin, N. M. Bogoliubov, and A. G. Izergin, *Quantum Inverse Scattering Method and Correlation Functions*. Cambridge Monographs on Mathematical Physics. Cambridge University Press, Cambridge, 1993.
- [54] J. Ruiz, *Differential Galois Theory and Non-Integrability of Hamiltonian Systems*. Progress in Mathematics. Springer Basel, 1999.
- [55] Y. Chervonyi and O. Lunin, *(Non)-Integrability of Geodesics in D-brane Backgrounds*, *JHEP* **02** (2014) 061, [[arXiv:1311.1521](#)].
- [56] P. Basu and L. A. Pando Zayas, *Analytic Non-integrability in String Theory*, *Phys. Rev. D* **84** (2011) 046006, [[arXiv:1105.2540](#)].
- [57] K. Hashimoto, K.-B. Huh, K.-Y. Kim, and R. Watanabe, *Exponential growth of out-of-time-order correlator without chaos: inverted harmonic oscillator*, *JHEP* **11** (2020) 068, [[arXiv:2007.04746](#)].
- [58] S. Grozdanov, K. Schalm, and V. Scopelliti, *Black hole scrambling from hydrodynamics*, *Phys. Rev. Lett.* **120** (2018), no. 23 231601, [[arXiv:1710.00921](#)].
- [59] V. Cardoso, A. S. Miranda, E. Berti, H. Witek, and V. T. Zanchin, *Geodesic stability, Lyapunov exponents and quasinormal modes*, *Phys. Rev. D* **79** (2009), no. 6 064016, [[arXiv:0812.1806](#)].
- [60] K. Goldstein, S. Kachru, S. Prakash, and S. P. Trivedi, *Holography of Charged Dilaton Black Holes*, *JHEP* **08** (2010) 078, [[arXiv:0911.3586](#)].
- [61] C. Charmousis, B. Gouteraux, B. S. Kim, E. Kiritsis, and R. Meyer, *Effective Holographic Theories for low-temperature condensed matter systems*, *JHEP* **11** (2010) 151, [[arXiv:1005.4690](#)].
- [62] B. Gouteraux and E. Kiritsis, *Generalized Holographic Quantum Criticality at Finite Density*, *JHEP* **12** (2011) 036, [[arXiv:1107.2116](#)].

- [63] B. Gouteraux and E. Kiritsis, *Quantum critical lines in holographic phases with (un)broken symmetry*, *JHEP* **04** (2013) 053, [[arXiv:1212.2625](#)].
- [64] J. L. Blázquez-Salcedo, X. Y. Chew, J. Kunz, and D.-H. Yeom, *Ellis wormholes in anti-de Sitter space*, *Eur. Phys. J. C* **81** (2021), no. 9 858, [[arXiv:2012.06213](#)].
- [65] J. Maldacena and A. Strominger, *Black Hole Greybody Factors and D-Brane Spectroscopy*, *Phys. Rev. D* **55** (1997) 861, [[hep-th/9609026](#)].
- [66] A. Strominger and C. Vafa, *Microscopic origin of the Bekenstein-Hawking entropy*, *Phys. Lett. B* **379** (1996) 99–104, [[hep-th/9601029](#)].
- [67] J. M. Maldacena, *The Large N limit of superconformal field theories and supergravity*, *Adv. Theor. Math. Phys.* **2** (1998) 231–252, [[hep-th/9711200](#)].
- [68] V. Balasubramanian and P. Kraus, *A Stress Tensor for Anti-de Sitter Gravity*, *Comm Math Phys* **208** (1999) 413–428, [[hep-th/9902121](#)].
- [69] G. W. Gibbons and C. M. Hull, *A Bogomolny Bound for General Relativity and Solitons in $N=2$ Supergravity*, *Phys. Lett. B* **109** (1982) 190–194.
- [70] J. Maldacena, J. Michelson, and A. Strominger, *Anti de-Sitter Fragmentation*, *JHEP* **02** (1999) 011, [[hep-th/9812073](#)].
- [71] V. Jahnke, K.-Y. Kim, and J. Yoon, *On the Chaos Bound in Rotating Black Holes*, *JHEP* **05** (2019) 037, [[arXiv:1903.09086](#)].
- [72] P. Banerjee, *Holographic Brownian motion at finite density*, *Phys. Rev. D* **94** (2016), no. 12 126008, [[arXiv:1512.05853](#)].
- [73] L. D. Landau and E. M. Lifshits, *Quantum Mechanics: Non-Relativistic Theory*, vol. v.3 of *Course of Theoretical Physics*. Butterworth-Heinemann, Oxford, 1991.
- [74] S. S. Gubser, *Momentum fluctuations of heavy quarks in the gauge-string duality*, *Nucl. Phys. B* **790** (2008) 175–199, [[hep-th/0612143](#)].
- [75] D. Giataganas and H. Soltanpanahi, *Universal Properties of the Langevin Diffusion Coefficients*, *Phys. Rev. D* **89** (2014), no. 2 026011, [[arXiv:1310.6725](#)].
- [76] D. Giataganas, *Stochastic Motion of Heavy Quarks in Holography: A Theory-Independent Treatment*, *PoS CORFU2017* (2018) 032, [[arXiv:1805.09011](#)].
- [77] J. Casalderrey-Solana and D. Teaney, *Transverse Momentum Broadening of a Fast Quark in a $N=4$ Yang Mills Plasma*, *JHEP* **04** (2007) 039, [[hep-th/0701123](#)].
- [78] J. Casalderrey-Solana, K.-Y. Kim, and D. Teaney, *Stochastic String Motion Above and Below the World Sheet Horizon*, *JHEP* **12** (2009) 066, [[arXiv:0908.1470](#)].
- [79] A. N. Atmaja, J. de Boer, and M. Shigemori, *Holographic Brownian Motion and Time Scales in Strongly Coupled Plasmas*, *Nucl. Phys. B* **880** (2014) 23–75, [[arXiv:1002.2429](#)].

- [80] M. Blake, R. A. Davison, and D. Vegh, *Horizon constraints on holographic Green's functions*, *JHEP* **01** (2020) 077, [[arXiv:1904.12883](#)].
- [81] T. Faulkner, H. Liu, J. McGreevy, and D. Vegh, *Emergent quantum criticality, Fermi surfaces, and AdS(2)*, *Phys. Rev. D* **83** (2011) 125002, [[arXiv:0907.2694](#)].
- [82] V. Cardoso and J. P. S. Lemos, *Scalar, electromagnetic and Weyl perturbations of BTZ black holes: Quasinormal modes*, *Phys. Rev. D* **63** (2001) 124015, [[gr-qc/0101052](#)].
- [83] E. Berti, V. Cardoso, and A. O. Starinets, *Quasinormal modes of black holes and black branes*, *Class. Quant. Grav.* **26** (2009) 163001, [[arXiv:0905.2975](#)].
- [84] S. S. Gubser, I. R. Klebanov, and A. M. Polyakov, *A Semiclassical limit of the gauge / string correspondence*, *Nucl. Phys. B* **636** (2002) 99–114, [[hep-th/0204051](#)].
- [85] S. Frolov and A. A. Tseytlin, *Semiclassical quantization of rotating superstring in AdS(5) x S**5*, *JHEP* **06** (2002) 007, [[hep-th/0204226](#)].
- [86] J. A. Minahan, *Circular semiclassical string solutions on AdS(5) x S(5)*, *Nucl. Phys. B* **648** (2003) 203–214, [[hep-th/0209047](#)].
- [87] A. Armoni, J. L. F. Barbon, and A. C. Petkou, *Rotating strings in confining AdS / CFT backgrounds*, *JHEP* **10** (2002) 069, [[hep-th/0209224](#)].
- [88] A. Armoni, J. L. F. Barbon, and A. C. Petkou, *Orbiting strings in AdS black holes and N=4 SYM at finite temperature*, *JHEP* **06** (2002) 058, [[hep-th/0205280](#)].
- [89] S. Frolov and A. A. Tseytlin, *Multispin string solutions in AdS(5) x S**5*, *Nucl. Phys. B* **668** (2003) 77–110, [[hep-th/0304255](#)].
- [90] S. Frolov and A. A. Tseytlin, *Rotating string solutions: AdS / CFT duality in nonsupersymmetric sectors*, *Phys. Lett. B* **570** (2003) 96–104, [[hep-th/0306143](#)].
- [91] N. Beisert, J. A. Minahan, M. Staudacher, and K. Zarembo, *Stringing spins and spinning strings*, *JHEP* **09** (2003) 010, [[hep-th/0306139](#)].
- [92] N. Beisert, S. Frolov, M. Staudacher, and A. A. Tseytlin, *Precision spectroscopy of AdS / CFT*, *JHEP* **10** (2003) 037, [[hep-th/0308117](#)].
- [93] J. Engquist, J. A. Minahan, and K. Zarembo, *Yang-Mills duals for semiclassical strings on AdS(5) x S(5)*, *JHEP* **11** (2003) 063, [[hep-th/0310188](#)].
- [94] G. Arutyunov and S. Frolov, *Integrable Hamiltonian for classical strings on AdS(5) x S**5*, *JHEP* **02** (2005) 059, [[hep-th/0411089](#)].
- [95] M. Smedback, *Pulsating strings on AdS(5) x S**5*, *JHEP* **07** (2004) 004, [[hep-th/0405102](#)].
- [96] M. Kruczenski, A. V. Ryzhov, and A. A. Tseytlin, *Large spin limit of AdS(5) x S**5 string theory and low-energy expansion of ferromagnetic spin chains*, *Nucl. Phys. B* **692** (2004) 3–49, [[hep-th/0403120](#)].

- [97] M. Alishahiha, A. E. Mosaffa, and H. Yavartanoo, *Multispin string solutions in AdS black hole and confining backgrounds*, *Nucl. Phys. B* **686** (2004) 53–74, [[hep-th/0402007](#)].
- [98] J. Plefka, *Spinning strings and integrable spin chains in the AdS/CFT correspondence*, *Living Rev. Rel.* **8** (2005) 9, [[hep-th/0507136](#)].
- [99] D. J. Gross and F. Wilczek, *Asymptotically free gauge theories. ii*, *Phys. Rev. D* **9** (Feb, 1974) 980–993.
- [100] B. Craps, M. De Clerck, P. Hacker, K. Nguyen, and C. Rabideau, *Slow scrambling in extremal BTZ and microstate geometries*, *JHEP* **03** (2021) 020, [[arXiv:2009.08518](#)].
- [101] D. Giataganas and K. Zoubos, *Non-integrability and Chaos with Unquenched Flavor*, *JHEP* **10** (2017) 042, [[arXiv:1707.04033](#)].
- [102] A. Zee, *Einstein Gravity in a Nutshell*. Princeton University Press, New Jersey, 5, 2013.

